# RAPSYN-Mediated Neddylation of BCR-ABL Alternatively Determines the Fate of Philadelphia Chromosome-positive Leukemia

Mengya Zhao[1†], Beiying Dai[2†], Xiaodong Li[1†], Yixin Zhang[2†], Chun Qiao[2, 3], Yaru Qin[2], Zhao Li[1], Qingmei Li[1], Shuzhen Wang[1*], Yong Yang[2*], Yijun Chen[1, 2, 4*]

[1]Laboratory of Chemical Biology, School of Life Science and Technology, China Pharmaceutical University, Nanjing, 211198, China

[2]State Key Laboratory of Natural Medicines, China Pharmaceutical University, Nanjing, 211198, China

[3]Department of Hematology, The First Affiliated Hospital of Nanjing Medical University, Jiangsu Province Hospital, Nanjing, 210029, China

[4]Chongqing Innovation Institute of China Pharmaceutical University, Chongqing 401135, China

[†] These authors contributed equally

***Correspondence**: Yijun Chen (yjchen@cpu.edu.cn), Yong Yang (yy@cpu.edu.cn) and Shuzhen Wang (shuzhenwang@cpu.edu.cn)

**Abstract**

Philadelphia chromosome-positive ($Ph^+$) leukemia is a fatal hematological malignancy. Although standard treatments with tyrosine kinase inhibitors (TKI) have achieved remarkable success in prolonging patient survival, intolerance, relapse and TKI resistance remain serious issues for patients with $Ph^+$ leukemia. Here, we report a new leukemogenic process in which RAPSYN and BCR-ABL co-occur in $Ph^+$ leukemia, and RAPSYN mediates the neddylation of BCR-ABL. Consequently, neddylated BCR-ABL enhances the stability by competing its c-CBL-mediated degradation. Furthermore, SRC phosphorylates RAPSYN to activate its NEDD8 E3 ligase activity, promoting BCR-ABL stabilization and disease progression. Moreover, in contrast to *in vivo* ineffectiveness of PROTAC-based degraders, depletion of RAPSYN expression or its ligase activity decreased BCR-ABL stability and, in turn, inhibited tumor formation and growth. Collectively, these findings represent an alternative to tyrosine kinase activity for the oncoprotein and leukemogenic cells and generate a rationale of targeting RAPSYN-mediated BCR-ABL neddylation for the treatment of $Ph^+$ leukemia.

## Introduction

Philadelphia chromosome-positive ($Ph^+$) leukemia is a myeloproliferative neoplasm characterized by the reciprocal translocation between the long arms of chromosome 9 and 22, t (9;22) (q34.1; q11.2) ( de Klein et al., 1982; Deininger et al., 2000). This cytogenetic abnormality results in a *BCR-ABL* fusion gene, which encodes the chimeric protein BCR-ABL with enhanced tyrosine kinase activity (Cortes et al., 2021). Based on its oncogenic role in $Ph^+$ leukemia, BCR-ABL has been regarded as the most pivotal target for $Ph^+$ leukemia therapy, especially for chronic myeloid leukemia (CML). Tyrosine kinase inhibitors (TKI) have been the main treatment option for $Ph^+$ leukemia, remarkably prolonging the patients' life span and improving their quality of life (Hochhaus et al., 2020; Jabbour and Kantarjian, 2020). However, most patients develop TKI resistance and relapse after long-term treatment (Braun et al., 2020). It is worth noting that the increase of BCR-ABL expression can affect the sensitivity to TKIs and eventually determine the rate of TKI resistance in patients with $Ph^+$ leukemia in addition to the mutations in the kinase domain (Jabbour et al., 2007). Mutations in the kinase domain can change the conformation of BCR-ABL, thus interfering with the binding between TKIs and BCR-ABL and resulting in decreased therapeutic efficacy (Lussana et al., 2018). In parallel, the increase of BCR-ABL expression can affect the sensitivity to TKIs and eventually determine the rate of disease progression and TKI resistance in patients with $Ph^+$ leukemia (Barnes et al., 2005). Therefore, effective degradation of BCR-ABL could address the issues on TKI resistance and leukemia-initiating cells (LICs), and PROTAC-based protein degradation strategy may represent a new therapeutic approach (Bekes et al., 2022). Currently, based on different ubiquitin E3 ligases, including VHL, CRBN and IAP, PROTAC-based degraders at nM level have shown significant degradation of BCR-ABL in CML cell lines, cell lines carrying mutations in BCR-ABL as well as patient-derived primary cells containing multiple BCR-ABL mutations ( Demizu et al., 2016; Lai et al., 2016; Shimokawa et al., 2017; Zhao et al., 2019; Burslem et al., 2019; Liu et al., 2022) . Unfortunately, the excellent cellular activity by the PROTAC-based degraders

has not been able to translate to *in vivo* efficacy, even in rare examples of xenografted mouse models ( Zhao, Ren et al., 2019; Jiang et al., 2021a), resulting in uncertain usefulness of these degraders. Nonetheless, the unsatisfactory results are not really surprising because the underlying mechanism of elevated BCR-ABL expression remains largely unclear.

Receptor-associated protein of the synapse (RAPSYN) has been identified as a classic synaptic adaptor protein that binds to the acetylcholine receptor (AChR) and several cytoskeleton-associated proteins, contributing to AChR clustering and neuromuscular junction (NMJ) formation (Huh and Fuhrer, 2002; Witzemann et al., 2013). Later, RAPSYN was found to exert NEDD8 E3 ligase activity to catalyze the neddylation for AChR aggregation.(Li et al., 2016) Despite the extensive studies of RAPSYN in muscular and neuronal cells and tissues (Legay and Mei, 2017; Li et al., 2018), with regard to its involvement in leukemogenesis, there is no available information thus far except for our previous finding. Previously, RAPSYN was found to be located in the cytosol of the typical $Ph^+$ leukemia cell line K562 when a small molecule was used to probe its binding proteins using a proteomics approach (Wang et al., 2015). Because of its newly identified E3 ligase activity for neddylation and its occurrence in the $Ph^+$ leukemia cell line, we speculated that RAPSYN might contribute to $Ph^+$ leukemia development through its enzymatic activity instead of only serving as a scaffolding protein.

As a type of post-translational modification (PTM), neddylation is sequentially catalyzed by the neuronal precursor cell-expressed developmentally downregulated protein 8 (NEDD8)-activating enzyme E1 (NAE1), NEDD8-conjugating enzyme E2 (UBE2M/UBC12 or UBE2F), and a substrate-specific NEDD8 E3 ligase to complete the covalent conjugation of NEDD8 to a lysine residue of its substrates ( van der Veen and Ploegh, 2012; Enchev et al., 2015). The neddylation of proteins can be reversed by deneddylases such as NEDP1. In the last two decades, accumulating evidence indicated the strong involvement of dysregulated neddylation in tumor progression, neurodegenerative and cardiac diseases, aberrant immunoregulation and others ( Ying

111 et al., 2018; Zhou et al., 2019; Li et al., 2020; Yao et al., 2020), which rationalizes the
112 modulation of neddylation as a feasible therapeutic strategy.

113 In this study, we report that RAPSYN is highly expressed along with BCR-ABL in
114 patients with Ph$^+$ leukemia and promotes disease progression, presumably by
115 stabilizing the BCR-ABL fusion protein *via* neddylation. The neddylation of BCR-ABL
116 by RAPSYN subsequently competes its ubiquitination-dependent degradation to
117 increase the stability of BCR-ABL. Additionally, the NEDD8 E3 ligase activity of
118 RAPSYN can be substantially increased by SRC-mediated phosphorylation, leading
119 to enhanced stability and activity of RAPSYN.

120 **Results**

121 **High protein levels of RAPSYN promoted Ph$^+$ leukemia progression**

122 Prior to investigating the biological roles of RAPSYN in the pathogenesis of Ph$^+$
123 leukemia, its expression at both mRNA and protein levels was analyzed. Neither a
124 publicly available database nor our collection of patient samples and cell lines showed
125 a significant increase in mRNA levels (Figure1-figure supplement 1A-C). The protein
126 levels of RAPSYN were substantially elevated in the peripheral blood mononuclear
127 cells (PBMC) of Ph$^+$ CML (#8-11) and the bone marrow of ALL (#7) patient samples in
128 comparison to that of healthy donors (#1-6), which was in a direct accordance with the
129 expression of BCR-ABL (Figure 1A). This co-expression of RAPSYN and BCR-ABL
130 was also found in Ph$^+$ cell lines (Figure 1B), suggesting that the function of RAPSYN
131 in Ph$^+$ leukemia could be closely related to BCR-ABL.

132 To examine the relationship between RAPSYN and Ph$^+$ leukemia progression, we
133 first performed knockdown of its expression by using shRNAs. Marked reduction of
134 RAPSYN levels and notable cytotoxicity were observed in all tested Ph$^+$ leukemia cells
135 transduced with RAPSN shRNAs (Figure 1C, Figure1-figure supplement 1D-F),
136 indicating the dependence on the presence and expression level of BCR-ABL.
137 Conversely, exogenous expression of RAPSN rescued Ph$^+$ leukemia cells from
138 shRNA-generated toxicity (Figure 1D). Knockdown of RAPSYN also changed the
139 phenotypes of Ph$^+$ leukemia cells, including proliferation, G0/G1 cell cycle arrest and

140 apoptosis (Figure 1E-G, Figure1-figure supplement 1G, H).

141 Next, we subcutaneously implanted empty body transduced sh*RAPSN*#3 or K562
142 cells into NCG mice to establish a cell line derived xenotransplantation mouse model
143 (Figure 1H). Tumor growth was significantly inhibited by RAPSYN silencing (Figure 1I,
144 J, Figure1-figure supplement 1I). Meanwhile, immunoblotting of tumor samples
145 showed a notable downregulation of RAPSYN expression, along with the reduction of
146 BCR-ABL levels (Figure 1K). After knockout of RAPSYN for remarkable depletion of
147 BCR-ABL expression in K562 cells (Figure 1L, Figure1-figure supplement 1K), these
148 cells along with the empty vector-transduced K562 cells were intravenously injected
149 into NCG mice to establish the leukemogenic mouse model (Figure 1H). Consequently,
150 the survival of tumor-bearing mice was profoundly prolonged by the knockout of
151 RAPSYN compared to the controls (Figure 1M). Altogether, our findings indicate that
152 RAPSYN is highly expressed at protein level with the accordance to BCR-ABL in $Ph^+$
153 leukemia and its depletion results in inhibiting the progression of $Ph^+$ leukemia.

154 **RAPSYN directly neddylated BCR-ABL**

155 Previous reports determined that both nicotinic AChR subunit $\alpha_7$ and muscarinic AChR
156 subtypes $M_2$, $M_3$, and $M_4$ were involved in the the cell proliferation of K562 cells
157 (Cabadak et al., 2011; Önder Narin et al., 2021). Furthermore, RAPSYN was found to
158 exert its NEDD8 E3 ligase activity toward AChR in neuronal systems (Li, Cao et al.,
159 2016). To determine whether RAPSYN functioned in a similar manner in leukemogenic
160 cells, we investigated whether RAPSYN promoted $Ph^+$ leukemia progression through
161 neddylation of AChRs. Despite AChR subunits $\alpha_7$, $M_2$, $M_3$, and $M_4$ were expressed in
162 all tested cells, no change in their neddylation was observed upon RAPSYN ablation
163 (Figure2-figure supplement 2A, B). On the basis of the co-expression of RAPSYN and
164 BCR-ABL, we postulated that RAPSYN could specifically mediate neddylation of BCR-
165 ABL to promote $Ph^+$ leukemia development.

166 To test this hypothesis, reciprocal immunoprecipitation was performed to reveal a
167 strong interaction between RAPSYN and BCR-ABL in $Ph^+$ leukemia cells (Figure 2A,
168 Figure2-figure supplement 2C). Similar results were obtained with exogenous

169 expression in HEK293T cells (Figure 2B), further confirming the specific interaction of
170 RAPSYN with BCR-ABL. Furthermore, GST pull-down assay with purified proteins
171 displayed specific binding of GST-tagged RAPSYN to His-tagged BCR-ABL (Figure
172 2C), indicating that BCR-ABL is the primary target of RAPSYN-mediated neddylation.
173 Domain mapping revealed that the Δ1 domain (1-927 aa) of BCR-ABL was responsible
174 for the interaction with RAPSYN (Figure 2D).

175 Next, we studied whether RAPSYN could directly mediate BCR-ABL neddylation.
176 Preeminent BCR-ABL neddylation was detected in all $Ph^+$ leukemia cell lines (Figure
177 2E, Figure2-figure supplement 2D). Treatment with the NAE1 inhibitor, MLN4924,
178 significantly dampened the neddylation of BCR-ABL (Figure 2F, Figure2-figure
179 supplement 2E). In addition, the mutation of two glycine residues at the C-terminus of
180 NEDD8 required for its covalent conjugating ability, or the co-expression of NEDP1
181 (NEDD8-specific protease 1) essentially diminished the neddylation of BCR-ABL
182 (Figure 2G, H). As shown in Figure 2I, we co-expressed either WT-RAPSYN or its
183 C366A mutant along with BCR-ABL and NEDD8, revealing that mutation of Cys to Ala
184 at the catalytic residue C366 significantly decreased the neddylation level of BCR-ABL.
185 Additionally, knockout of RAPSYN abrogated BCR-ABL neddylation in the cells, and
186 this effect was restored by transduction of *RAPSN* cDNA (Figure 2J). These results
187 were further corroborated by *in vitro* experiments, which showed that BCR-ABL could
188 hardly be neddylated in the absence of RAPSYN (Figure 2K). Consistently, the amount
189 of neddylated BCR-ABL was markedly reduced in tumors generated by K562 cells
190 transfected with sh*RAPSN*#3 (Figure 2L), indicating an essential role of the ligase
191 activity of RAPSYN in BCR-ABL neddylation.

192 In addition, neither overall BCR-ABL expression nor its neddylation levels were
193 affected after the knockdown of AChRs (Figure2-figure supplement 2F). Similarly,
194 modulation of AChR activities and their downstream PKC-RAS-ERK and JAK2-AKT
195 signaling pathways ( Kawamata et al., 2011; Aydin et al., 2013) by either an agonist
196 (carbachol) (Jakubik et al., 2008) or antagonists (benzethonium and homatropine)
197 (Durieux and Nietgen, 1997) did not alter the expression or neddylation status of BCR-

198 ABL (Figure2-figure supplement 2G, H).

199 Subsequently, we tried to identified specific modification sites on BCR-ABL. The
200 purified proteins were used for *in vitro* neddylation reactions, and the target bands were
201 digested with trypsin for LC-MS/MS analyses. Eight lysine residues were found to be
202 potential NEDD8 accepting sites in BCR-ABL (Figure2-figure supplement 3). To
203 confirm these modification sites, a series of individual Lys-to-Arg mutants were
204 generated. Except for K257, neddylation levels of BCR-ABL at other candidate sites
205 were all significantly reduced, confirming the modification sites of these Lys residues
206 (Figure 2M).

207 **RAPSYN attenuated c-CBL-mediated BCR-ABL ubiquitination and degradation**

208 As decreased neddylation of BCR-ABL following either MLN4924 treatment or
209 RAPSYN/KO was accompanied by a strong decline in its overall protein expression
210 level (Figure 2F, 3A-B, Figure2-figure supplement 2E, 4), we asked whether RAPSYN-
211 mediated BCR-ABL neddylation affects protein stability. Subsequently, the protein
212 synthesis inhibitor CHX was applied to K562 cells transduced with vectors encoding
213 doxycycline-inducible *RAPSN* shRNA #3. Indeed, the expression levels of BCR-ABL
214 declined much faster in cells with the induction of shRNA expression (Figure 3C).
215 Meanwhile, we found that a clear inverse correlation between the neddylation and
216 ubiquitination levels of BCR-ABL was observed (Figure 3D, E). BCR-ABL ubiquitination
217 was remarkably reduced in the cells transfected with NEDD8 (Figure 3F). Consistent
218 with these results, treatment of the cells with the proteasome inhibitor MG132
219 significantly increased the amount of ubiquitinated BCR-ABL accompanied by the
220 decrease of BCR-ABL neddylation (Figure 3G).

221 To clarify the molecular basis of the battle between BCR-ABL neddylation and its
222 ubiquitination, we detected that whether RAPSYN competes for binding to BCR-ABL
223 with c-CBL, a reported E3 ligase mediating BCR-ABL ubiquitin-proteasome
224 degradation (Mao et al., 2010). As a result, exogenous expression of RAPSYN
225 interfered with the interactions between BCR-ABL and c-CBL, whereas RAPSYN
226 ablation in K562 cells promoted c-CBL binding to BCR-ABL (Figure 3H, I). These data

227 indicate that RAPSYN competes with c-CBL for binding to BCR-ABL, leading to
228 subsequent BCR-ABL neddylation to enhance BCR-ABL stability by counteracting its
229 proteasomal degradation.

230 **SRC-mediated phosphorylation stabilized RAPSYN by repressing its**
231 **proteasomal degradation**

232 SRC-family protein tyrosine kinases are capable of phosphorylating RAPSYN in
233 neuronal system, among which SRC exerts the strongest function (Mohamed and
234 Swope, 1999). In addition, SRC has been shown to be highly expressed in primary
235 CML cells (Yang et al., 2017). We then studied whether SRC acts as an upstream
236 regulator to mediate RAPSYN. SRC inhibition with saracatinib or shRNA not only
237 significantly downregulated phosphorylated (Tyr418) SRC, but also inhibited the
238 phosphorylation of endogenous RAPSYN, resulting in a substantial decline in its
239 protein level, whereas heterologous expression of *SRC* increased RAPSYN
240 phosphorylation (Figure 4A-C, Figure4-figure supplement 5A). Furthermore, *in vitro*
241 incubation with recombinant RAPSYN, SRC, and ATP resulted in strong
242 phosphorylation of RAPSYN, which could be fully abrogated by saracatinib treatment
243 (Figure 4D). LC-MS/MS analyses indicated that Tyr residues at positions 59, 152, and
244 336 in RAPSYN are potential phosphorylation sites by SRC (Figure4-figure
245 supplement 5B). Then, after mutagenesis of these sites from Tyr to Phe, Y336, an
246 evolutionarily conserved Tyr residue, was confirmed to be the primary site of RAPSYN
247 phosphorylation (Figure 4E, Figure4-figure supplement 5C). As SRC has no effect on
248 *RAPSN* mRNA levels (Figure4-figure supplement 5D, E), implying that SRC-mediated
249 phosphorylation also affects RAPSYN stability. In fact, $Ph^+$ leukemia cells were treated
250 with saracatinib, SRC silencing or mutation of the key phosphorylation site significantly
251 accelerated the diminishment of RAPSYN expression following CHX treatment,
252 conversely, expressing exogenous SRC cDNA prolonged the half-life of RAPSYN
253 (Figure 4F-I).

254 To explore the molecular mechanisms responsible for the increased stability of
255 phosphorylated RAPSYN, $Ph^+$ leukemia cells were treated with saracatinib or

transduction of sh*SRC* followed by incubation with MG132. In all circumstances, MG132 could rescue the decrease of RAPSYN induced by saracatinib treatment or sh*SRC* knockdown (Figure 4J, K). Clearly, the specific phosphorylation of RAPSYN at Y336 by SRC led to its increased stability by preventing the proteasomal degradation, thereby maintaining the high levels of RAPSYN in $Ph^+$ leukemia.

**Phosphorylated RAPSYN potentiated its NEDD8 E3 ligase activity and promoted BCR-ABL stabilization**

To dissect the role of SRC-mediated phosphorylation of RAPSYN, we tested whether phosphorylation of RAPSYN at Y336 affects its ligase activity. Immunoblotting revealed saracatinib treatment or SRC silencing reduced BCR-ABL neddylation and its protein expression, while exogenous expression of *SRC* cDNA strongly increased it (Figure 5A-C). Additionally, co-expression in HEK293T cells showed that Y336F mutation had no impact on BCR-ABL neddylation compared to co-transfection with SRC (Figure 5D). These results were supported by stronger neddylation of endogenous BCR-ABL in cells overexpressing WT RAPSYN, but not in the Y336F mutant (Figure 5E). Furthermore, protein turnover rates of BCR-ABL were determined in $Ph^+$ leukemia cells and the cells with exogenous $RAPSN^{Y336F}$ expression displayed larger decrease in BCR-ABL level than those expressing $RAPSN^{WT}$ (Figure 5F). Therefore, RAPSYN phosphorylation at Y336 by SRC was a major contributing factor to its NEDD8 E3 ligase activity and BCR-ABL stability in $Ph^+$ leukemia cells.

**Phosphorylation of RAPSYN at Y336 promoted $Ph^+$ leukemia progression**

To assess the extent to which SRC-mediated phosphorylation of RAPSYN at Y336 contributes to the enhanced viability of RAPSYN-dependent $Ph^+$ leukemia cells, we first identified a specific sh*SRC* by screening five candidates using toxicity tests and then performing rescue experiments with *SRC* cDNA. Toxicity tests revealed that, albeit to varying degrees, sh*SRC*#2, #4, and #5 induced cytotoxicity in all $Ph^+$ leukemia cell lines (Figure 6A, Figure6-figure supplement 6A). However, exogenous *SRC* cDNA expression only restored the growth of $Ph^+$ leukemia cells transduced with sh*SRC*#2 (Figure 6B, Figure6-figure supplement 6B, C).

285 Subsequently, we performed rescue experiments by introducing *RAPSN*$^{WT/Y336F}$
286 cDNA or an empty vector into shSRC#2-transducted Ph$^{+}$ leukemia cells and found that
287 virtually complete *RAPSN*$^{WT}$-induced rescue was detected in both cell lines, but
288 *RAPSN*$^{Y336F}$ exhibited no restoring effect (Figure 6C, D). In addition, transduction of
289 *RAPSN*$^{WT}$ cDNA conferred an increased resistance against saracatinib treatment,
290 whereas the expression of *RAPSN*$^{Y336F}$ cDNA did not affect the drug sensitivity of the
291 cells (Figure 6E, F). Furthermore, knockdown of RAPSYN substantially sensitized both
292 cell lines to saracatinib (Figure 6G).

293 In animal models, while the overall survival of mice intravenously injected with
294 K562 cells expressing control empty vector was significantly improved by either
295 saracatinib administration or shRNA-mediated SRC inhibition, overexpression of WT
296 RAPSYN fully counteracted these effects and shortened the lifespan of mice to the
297 levels comparable to those of mice injected with K562 cells without SRC inhibition. In
298 contrast, expression of exogenous *RAPSN*$^{Y336F}$ attenuated the protective effects of
299 SRC inhibition to a much lesser extent (Figure 6H-J). Taken together, these results
300 suggest that phosphorylation at Y336 by SRC is a major event in the pro-leukemogenic
301 functions of RAPSYN in Ph$^{+}$ leukemia development.

302 **Discussion**

303 In this study, we identified a novel role of RAPSYN in hematology. Indeed,
304 RAPSYN inhibition significantly suppressed the survival of Ph$^{+}$ leukemia. This
305 phenotype was found to be linked to the NEDD8 E3 ligase activity of RAPSYN, which
306 mediated BCR-ABL neddylation to enhance its stability for promoting leukemogenesis
307 (Figure 7).

308 Balanced protein synthesis and degradation are pivotal for maintaining protein
309 homeostasis and normal cellular function. Currently, a variety of degraders for BCR-
310 ABL by PROTAC strategy have been reported ( Demizu, Shibata et al., 2016; Lai,
311 Toure et al., 2016; Shimokawa, Shibata et al., 2017; Zhao, Ren et al., 2019; Burslem,
312 Schultz et al., 2019; Liu, Mi et al., 2022;), and this approach for the degradation of
313 BCR-ABL has appeared to be effective on overcoming drug-resistance in various cell

314 lines (Demizu, Shibata et al., 2016; Jiang, Wang et al., 2021a). However, very few
315 reports with *in vivo* data in animal models have shown that the efficacy is way far from
316 satisfactory ( Zhao et al., 2019; Jiang et al., 2021a), due likely to the inherited
317 limitations of the degraders, such as unfavored physiochemical properties, significant
318 off-target effects, various safety issues and others (Li and Song, 2020; Bekes, Langley
319 et al., 2022). On the other hand, neddylation is a crucial type of PTM that modifies
320 multiple Lys residues in BCR-ABL, competing with and shielding this oncoprotein from
321 ubiquitination-mediated degradation, which provides a reasonable explanation on the
322 poor *in vivo* efficacy of PROTAC-based degraders for BCR-ABL. Meanwhile,
323 accumulating evidence has shown that targeting the neddylation process could be an
324 appealing strategy for anticancer therapy (Bhalla and Fiskus., 2016; McGrail et al.,
325 2020; Norton et al., 2021; Xie et al., 2021). MLN4924, a NEDD8-activating E1
326 enzyme inhibitor, has been shown to inhibit the survival of both wild-type (WT) and
327 T315I-BCR-ABL leukemia cells as well as leukemia-initiating cells ( Liu et al., 2018;
328 Bahjat et al., 2019; Guo et al., 2019). Moreover, clinical trials of MLN4924 in
329 combination with anticancer agents in acute myeloid leukemia (AML) have progressed
330 to phase II (NCT03745352 and PEVENAZA [NCT04266795]) and III
331 (PANTHER[NCT03268954] and PEVOLAM[NCT04090736]). However, the
332 neddylation system works in a substrate- and context-dependent manner, which
333 essentially defines its role in tumorigenesis as anti or pro, particularly relying on the
334 substrate specificity of the NEDD8 E3 ligase. Neddylation can either facilitate
335 ubiquitination-dependent degradation of its substrates, such as EGFR (Oved et al.,
336 2006) and c-SRC (Lee et al., 2018), or enhance protein stability in the cases of HuR
337 (Embade et al., 2012) and TGF-β type II receptor (Zuo et al., 2013). Thus, the antitumor
338 effects of MLN4924 are the integrative outcome of inhibiting more *pro*- than *anti*-
339 tumorigenic neddylation activities in the reported tumor types. Recent studies
340 uncovered that neddylation could also inhibit tumor progression and MLN4924
341 stimulates tumor sphere formation and wound healing as well as promotes glycolysis
342 (Zhou et al., 2016; Zhou, Jiang et al., 2019; Zhou and Sun, 2019). Therefore, rather

343 than suppressing the entire neddylation system to affect a wide range of proteins,
344 targeted inhibition of substrate-specific NEDD8 E3 ligase, such as RAPSYN, might
345 offer a potential therapeutic opportunity for more elegant anticancer intervention with
346 fewer side effects.

347 Functional studies on RAPSYN have focused on its contribution to neuromuscular
348 transmission (Xing et al., 2019; Xing et al., 2020). To date, whether RAPSYN is
349 involved in biological processes other than the formation and maintenance of NMJ
350 remains poorly understood. In this study, we found that RAPSYN promoted disease
351 progression by neddylating BCR-ABL for its resistance to c-CBL-mediated
352 proteasomal degradation. Intriguingly, although AChRs, the primary substrates of
353 RAPSYN E3 ligase activity in neural and muscle cells, were also found to be expressed
354 in $Ph^+$ leukemia cells, they were not identified as substrates of RAPSYN for neddylation,
355 suggesting highly orchestrated tissue-specificity of the RAPSYN enzymatic activity on
356 its substrates.

357 It is well known that the generation of BCR-ABL fusion protein is a decisive
358 characteristic of $Ph^+$ leukemia (de Klein et al., 1982). Aside from the occurrence of
359 RAPSYN in patients with $Ph^+$ leukemia, the present study revealed a fascinating
360 finding that BCR-ABL expression levels were correlated with those of RAPSYN,
361 demonstrating the specificity of RAPSYN-mediated neddylation of BCR-ABL.
362 Moreover, as a new type of PTM for BCR-ABL, RAPSYN-mediated neddylation was
363 found to compete c-CBL-mediated ubiquitination, causing a reduction in BCR-ABL
364 degradation. Given the fact that the increase of BCR-ABL expression can affect the
365 sensitivity to TKIs and eventually determine the rate of TKI resistance and LIC
366 population in patients with $Ph^+$ leukemia ( Issaad et al., 2000; Barnes, Palaiologou et
367 al., 2005), effective degradation of BCR-ABL is an alternative opportunity for the
368 treatment. Although recent studies have greatly advanced our understanding of the
369 regulation of BCR-ABL degradation (Burslem, Schultz et al., 2019; Shibata et al., 2020;
370 Jiang et al., 2021b), most reported modulatory proteins are not ideal for translation to
371 clinical settings because of their pivotal roles in sustaining normal hematological

functions. In contrast, RAPSYN was nearly unexpressed in the blood of healthy donors. Thus, it is reasonable to expect that the inhibition of RAPSYN expression could lead to cytotoxicity in $Ph^+$ leukemia with high specificity and marginal side effects. Furthermore, our present results showed that knockdown of RAPSYN significantly increased the sensitivity of leukemia cells to saracatinib, implying that a combination of RAPSYN inhibition and TKI treatment can effectively control mutations and LIC-derived TKI resistance in $Ph^+$ leukemia.

In summary, our work has uncovered the pivotal role that RAPSYN exerts its NEDD8 E3 ligase activity in neddylating and stabilizing BCR-ABL in the pathogenesis of $Ph^+$ leukemia and thus delineate it as a potential novel therapeutic target for the treatment of $Ph^+$ leukemia. More importantly, our results shed a light on future investigations that may help to extend to other cancer types for broadening our understanding of RAPSYN's involvement in hematology and oncology.

## Materials and Methods

### Human clinical samples

This study was approved by the ethics committee of the First Affiliated Hospital of Nanjing Medical University (2019-SR-485.A1). Human peripheral blood samples were obtained from the remaining material utilized for routine laboratory tests at the First Affiliated Hospital of Nanjing Medical University (Nanjing, China) and derived from 21 patients with $Ph^+$ chronic myeloid leukemia (CML), and six healthy volunteers. And one human bone marrow sample of $Ph^+$ acute lymphoblastic leukemia patient was obtained from the remaining material utilized for routine laboratory tests at the First Affiliated Hospital of Nanjing Medical University (Nanjing, China). Peripheral blood and bone marrow mononuclear cells were isolated by density gradient centrifugation using the Ficoll® Paque Plus solution (17-1440-02, GE Healthcare).

### Cell culture

K562 (female; CBP60529), MEG-01 (male; BP61104), and KU812 (male; BP60732) cells were purchased from COBIOER and cultured in Roswell Park Memorial Institute 1640 medium (RPMI 1640; KGM31800, KeyGEN BioTECH) containing 10-20% fetal bovine serum (FBS; FS301-02, TransGen Biotech) and 100 mg/mL streptomycin/penicillin (FG101-01, TransGen

Biotech). HS-5 (male; CRL11882, ATCC), purchased from the American Type Culture Collection (ATCC) and HEK293T (KG405) from KeyGEN BioTECH were cultured in Dulbecco's modified Eagle's medium (DMEM; KGM12800, KeyGEN BioTECH) containing 10% FBS and 100 mg/mL streptomycin/penicillin. All cells were cultured in a humidified incubator with 5% CO2 at 37°C. All the cell lines were authenticated using short tandem repeat matching analysis and tested negative for mycoplasma contamination.

**Animal studies**

Female NOD/ShiLtJGpt-Prkdcem26Cd52Il2rgem26Cd22/Gpt (NCG) mice (6-8 weeks), purchased from GemPharmatech Co., Ltd., were used for all in vivo studies. Mice were housed under specific pathogen-free conditions at 24 ± 1°C and 55 ± 5% humidity in a barrier facility with 12-h light-dark cycles. All animal experiments were performed in accordance with the National Institutes of Health Guide for the Care and Use of Laboratory Animals with the approval of the Center for New Drug Evaluation and Research, China Pharmaceutical University (approval number: B20190925-1; Nanjing, China).

**Apoptosis assay**

A total of 1-5 x $10^5$ cells were washed with phosphate-buffered saline (PBS; 02-024-1ACS, Biological Industries) and resuspended in 100 μL of 1 × Annexin V binding buffer (E-CK-A211, Elabscience). The cell suspension was incubated with 2.5 μL of Annexin V-AF647 (E-CK-A211, Elabscience) and 2.5 μL of propidium iodide (PI; E-CK-A211, Elabscience) for 20 min in the dark, followed by the addition of 400 μL of 1 × Annexin V binding buffer, and detection by flow cytometry (Thermo Attune NxT, MA, USA).

**Cell viability assay**

Cells were seeded at a density of 5,000 (K562) or 20,000 cells (MEG-01) per well in round-bottom 96-well plates and incubated with different concentrations of saracatinib (AZD0530, Selleck) or the corresponding amount of solvent for 72 h. Cells were then transferred to flat-bottom 96-well plates for the determination of cell viability using the CCK-8 Cell Counting Kit (A311-01, Vazyme) following the manufacturer's instructions. Each experiment was performed at least three times for each cell line.

**Cell proliferation assay**

Cells were washed twice with PBS, resuspended with a cell number of 2 x 106 in 1 mL PBS, and incubated with 2.5 μM carboxyfluorescein succinimidyl ester (CFSE) solution (1948076, Thermo Scientific) or 5 μM carboxylic acid, acetate, and succinimidyl ester (SNARF-1) solution (S-22801, Invitrogen) for 20 min at 37°C in the dark, respectively. Subsequently, 1 mL of FBS was added to stop the staining, and the cells were washed twice with complete media. Cell division was monitored by measuring CFSE or SNARF-1 dilution using flow cytometry via channels BL1 and YL1.

**Cell cycle analysis**

A total of 1×106 cells were washed once with pre-chilled PBS, fixed in ice-cold 70% ethanol, vortexing and kept for at least 20 min at -20°C. The fixed cells were washed twice with PBS and stained with 20 μg/mL propidium iodide (PI) containing 100 mg/mL RNAse A (740505, MACHEREY-NAGEL) for 15 min at room temperature. Stained nuclei were analyzed by flow cytometry and quantified using FlowJo software (BD Biosciences, NJ, USA).

**Cell transfection and viral transduction**

Transfection of the indicated DNA plasmids into HEK293T cells was performed using Lipofectamine 2000 (11668500, Thermo Fisher Scientific), according to the manufacturer's instructions. Briefly, transfection of HEK293T was performed when cell confluency reached 60-70%. Plasmids and Lipofectamine 2000 reagent were diluted in Opti-MEM medium (31985-070, Thermo Fisher Scientific) and incubated for 5 min at room temperature. They were then mixed together, incubated for another 20 min at room temperature, and added to the target cells. The transfected cells were collected after 48 h for further analysis.

**GST pull-down assay**

Purified GST or GST-RAPSYN (GenBank: NM_005055.5; 1236 bp ORF sequence) proteins were incubated with glutathione beads 4FF (SA010010, Smart-Lifescience) overnight at 4°C in binding buffer (0.14 M NaCl, 2.68 mM KCl, 2 mM KH2PO4, 0.01 M Na2HPO4, 10 mM DTT, pH 7.4), respectively, and incubated with purified His-BCR-ABL (p210 BCR-ABL (b3a2); 6126 bp ORF sequence) protein for another 4 h at 4°C. Beads were washed three times with washing buffer(0.14 M NaCl, 2.68 mM KCl, 2 mM KH2PO4, 0.01 M Na2HPO4, 0.5 mM reduced GSH, 10 mM DTT, pH 7.4), eluted with elution buffer(0.14 M NaCl, 2.68 mM KCl, 2mM KH2PO4,

0.01M Na2HPO4, 10 mM reduced GSH, 10mM DTT, pH 7.4), and subjected to immunoblotting detection.

**Immunoblotting**

The cells were lysed on ice with Nonidet® P-40 (NP-40) lysis buffer (150 mM NaCl, 100 mM NaF, 50 mM Tris-HCl (pH 7.6), and 0.5% NP-40) supplemented with a protease inhibitor cocktail (78446, Thermo Fisher Scientific). Lysates were centrifuged, quantified, subjected to sodium dodecyl sulfate-polyacrylamide gel electrophoresis (SDS-PAGE), and transferred to polyvinylidene difluoride (PVDF) membranes using a Bio-Rad transfer apparatus. Membranes were blocked with 5% non-fat milk in Tris-buffered saline buffer containing 0.1% Tween-20 (TBST) at 20-25°C for 2 h, followed by incubation with primary antibody overnight at 4°C. The membranes were then washed three times in TBST buffer and incubated with species-specific HRP-conjugated secondary antibodies for 2 h at room temperature. Afterwards, the membranes were washed three times in TBST buffer, developed using the enhanced chemiluminescence (ECL) reagent, and exposed to the ChemiDoc Imaging System (Tanon, Shanghai, China).

**Immunoprecipitation**

Immunoprecipitation assays were performed in accordance with the manufacturer's instructions. Briefly, the cells were lysed on ice with NP-40 lysis buffer supplemented with a protease inhibitor cocktail. Cell lysates were centrifuged, quantified, and incubated with the appropriate primary antibody overnight at 4°C, and subsequently with protein A agarose beads (16-125, Millipore) for another 4 h at 4°C. Agarose was washed three times with lysis buffer and eluted with SDS-PAGE loading buffer. The eluted immunocomplexes were separated by SDS-PAGE and transferred to PVDF membranes, which were probed with primary and corresponding secondary antibodies, washed three times in TBST buffer, developed using the ECL reagent, and exposed to the ChemiDoc Imaging System.

***In vitro* neddylation assay**

A 30 μL reaction mixture containing 2 mM ATP-Mg2+ (B-20, R&D), 50 ng E1(APPBP1/UBA3; E-313-25, R&D), 400 ng E2 (UBE2M; E2-656-100, R&D), 0.25 μg NEDD8 (UL-812-500, R&D),

0.35 μg His-BCR-ABL, with or without 4.77 μg RAPSYN was incubated at 37°C for 4 h. Reaction was terminated with SDS-PAGE loading buffer and assayed using immunoblotting.

**_In vitro_ phosphorylation assay**

A 40 μL reaction mixture containing 2 mM ATP-Mg2+, 3 μg RAPSYN, and 1 μg SRC (GenBank: NM_005417.5; 1608 bp ORF sequence) protein, with or without 2 μM saracatinib (AZD0530, Selleck), was incubated at 30°C for 30 min. Reaction was terminated with SDS-PAGE loading buffer and assayed using immunoblotting.

**Animal experiments with mouse models**

Female NCG mice aged 6-8 weeks were used in all the animal experiments. In the subcutaneous tumor experiment shown in Figure 1G, 20 mice were randomly divided into two groups, followed by subcutaneous injection of 1×106 K562-shNC or K562-shRAPSYN #3 cells in 60 μL Matrigel (354234, Corning) into the right foreleg. Tumor size was measured every two days using a digital caliper. The tumor volume was quantified using the following equation: tumor volume = 0.5 × (long diameter) × (short diameter) 2. When the average volume of the control group exceeded 2,000 mm3, the mice were sacrificed. The tumors were separated, and their weights were measured. As shown in the survival experiment in Figure 1J, NCG mice were inoculated with K562-RAPSYNWT or K562-RAPSYNKO (1×107 cells/mouse) via the tail vein. The survival time was recorded until the mice died. As shown in the survival experiment of Figure 6I, 40 mice were randomly divided into 4 groups and intravenously inoculated with K562-OE-NC (20 mice), K562-OE-RAPSYNWT (10 mice), or K562-OE-RAPSYNY336F (10 mice). From day 6 to 26 after tumor inoculation, 10 mice inoculated with K562-OE-NC were treated with vehicle orally, while the other 30 mice inoculated with K562-OE-NC, K562-OE-RAPSYNWT, or K562-OE-RAPSYNY336F, 10 mice in each group, were administered saracatinib orally (50 mg/kg/d). The survival time was recorded until the mice died. In the survival experiment shown in Figure 6J, 40 mice were randomly divided into four groups and intravenously inoculated with double-transfected K562 cells, as indicated. The survival time was recorded until the mice died.

**Identification of modification sites**

To determine which lysines in BCR-ABL were neddylated using NEDD8, a neddylation reaction (50 μL) was performed. After incubation at 37°C for 4 h, the reaction was run on an SDS-PAGE gel, silver-stained bands were excised and sent to BiotechPack Scientific Co., Ltd (Beijing, China) for liquid chromatography-mass spectrometry (LC-MS/MS) analysis. To determine which tyrosines in RAPSYN were phosphorylated by SRC, a phosphorylation reaction (50 μL) was performed. After a 30 min reaction was run on an SDS-PAGE, silver-stained bands were excised and sent to Applied Protein Technology Co., Ltd. (Shanghai, China) for liquid chromatography-mass spectrometry (LC-MS/MS) analysis.

**Plasmid construction**

Eukaryotic expression vectors encoding His-, GST-, HA-, Myc-, or Flag-tagged proteins were generated by inserting PCR-amplified fragments into the pcDNA3.1(+) mammalian expression vector (V79020, Invitrogen). Eukaryotic expression vectors encoding green fluorescent protein (GFP)-tagged proteins were generated by inserting PCR-amplified fragments into the pd1-EGFP-N1 vector (6073-1, Clontech). Prokaryotic plasmids encoding GST-fusion proteins were constructed using the pGEX-4T-1 bacterial expression vector (27-4580-01, Addgene). Mutants of His-, HA- GST-, or GFP-tagged proteins were generated using the QuickMutation Site-Directed Mutagenesis Kit (D0206, Beyotime) according to the manufacturer's instructions. Briefly, whole plasmid DNA was amplified by polymerase chain reaction (PCR) for 20 cycles with specific mutant primers (Supplemental Table S1) using the QuickMutation site-directed mutagenesis kit. Next, 1 μL DpnI was directly added to the PCR reaction mixture, followed by incubation at 37°C for 30 min and transformation. To verify the mutation sites, single clones were selected for DNA sequencing.

**Preparation of stable K562 RAPSYN KO cell line**

K562 RAPSYN KO cells were generated using the CRISPR/Cas9 system (Genloci Biotechnologies Inc.). RAPSYN single guide RNAs (sgRNAs) were designed using the online CRISPR design tool (http://crispr.mit.edu/). The sgRNA sequences were ATGGGGCGCTTCCGCGTGCTGGG, GTAGCGGCCCATCTCCGAGTGGG, and TCTGGTTGGACTGGTACAGCTGG, which were cloned into the pGK1.1/CRISPR/Cas9 vector (Genloci Biotechnologies Inc.). To obtain single clones of RAPSYN KO cells, K562 cells were

transfected with the pGK1.1/CRISPR/Cas9 plasmid containing the aforementioned sgRNA sequence, expanded, selected with puromycin (0120A21, LEAGENE), and isolated by single-cell culture. Single clones obtained from RAPSYN KO cells were validated by DNA sequencing and immunoblotting.

**Preparation of stable RAPSYN KD and SRC KD cell lines**

Lentivirus-producing shRNA targeting either human RAPSYN or SRC mRNA was used to inhibit endogenous RAPSYN or SRC expression, respectively. All shRNAs (Supplemental Table S1) were designed using online shRNA design tools (https://rnaidesigner.thermofisher.com and https://portals.broadinstitute.org). The shRNA primers were ordered from GenScript and annealed in a thermal cycler according to the following procedure (95°C, 2 min; 85°C, 9 min; 75°C, 9 min; 65°C, 9 min; 55°C, 9 min; 45°C, 9 min; 35°C, 9 min; 25°C, 10 min; 4°C, hold) with the presence of NEBuffer 2.1 (B7202S, NEW ENGLAND BioLabs) to form a double strand with EcoRI and AgeI sticky ends. Using T4 DNA ligase (M0202L, NEW ENGLAND BioLabs), the double-stranded shRNAs were ligated into either the lentiviral backbone plasmid vector pLKO-EGFP-puro or a tet pLKO-EGFP-puro, which was digested with the restriction enzymes EcoRI-HF (R3101S, NEW ENGLAND BioLabs) and AgeI-HF (R3552S, NEW ENGLAND BioLabs). Plasmids containing shRNA or the corresponding empty vector were cotransfected with lentivirus packaging plasmids (pLP1, pLP2, and pLP/VSVG) into HEK293T cells using the linear polyethylenimine (23966, Polyscience) transfection method. After transfection for 6–8 h, the transfection reagent was replaced with a fresh medium. After incubation at 37°C, 5% CO2 for 48 and 72 h, the resulting lentivirus supernatant was collected, respectively, and filtrated through a 0.22 μm disc filter. Then, 15 mL of the filtered lentivirus supernatant was concentrated through a 100 kD ultrafiltration tube at 1,500 × g and 4°C for 1 h. Ph+ leukemia cell lines were infected with concentrated lentivirus supernatant containing 8 μg/mL polybrene (H9268, Sigma). The culture plate or dish was centrifuged in a horizontal rotor centrifuge at 2,000 × g and 32°C for 1.5 h. After 48 h, the viral particles were replaced with fresh medium and 3 μg/mL puromycin was added for selection for another 48–72 h. Protein expression levels were analyzed by

immunoblotting with anti-RAPSYN (ab118491, Abcam) or SRC (11097-1-AP, Proteintech) antibodies.

**Preparation of stable RAPSYN WT，RAPSYNY 336F, or SRC expression cell lines**

Lentiviruses overexpressing RAPSYN WT, RAPSYN Y336F, or SRC were purchased from GenePharma. The volume of virus required was calculated using the following equation: Ph+ leukemia cell lines were infected using the spin-infection method described above. 48 h after infection, the viral particles were replaced with fresh medium. Stable RAPSYN WT, RAPSYNY 336F, or SRC expressing cells were selected in the presence of 3 μg/mL puromycin for 48-72 h. Protein expression levels were analyzed by immunoblotting with anti-RAPSYN or SRC antibodies.

$$\text{virus volume} = \frac{\text{MOI} \times \text{cell number}}{\text{virus titer}}$$

**Protein expression and purification**

Recombinant pGEX-4T-1-GST-RAPSYN plasmid were transformed into the ArcticExpress (DE3) pRARE2 competent cells (AYBIO-G6023, ANGYUBIO) and treated with 0.4 mM isopropyl-β-D-thiogalactoside (367-93-1, Sangon Biotech) to induce fusion protein expression under 8°C culture condition. After 50 h, cells were harvested, resuspended in PBS (0.14 M NaCl, 2.68 mM KCl, 2mM KH2PO4, 0.01M Na2HPO4, 10 mM DTT, pH 7.4), and sonicated on ice. Precipitates were removed from the cell lysates by centrifugation. Recombinant GST-RAPSYN was purified from the supernatant by GST-affinity chromatography (SA010010, Smart-Lifescience) and size-exclusion chromatography (17-0060-01, GE Healthcare). Purified GST-RAPSYN protein was digested with thrombin (T8021, Solarbio) for 6 h at 4°C to remove the GST tag. Recombinant pcDNA3.1-His-BCR-ABL plasmids were transfected into HEK293T cells, which were collected after 48 h and lysed on ice using Nonidet P-40 (NP-40) lysis buffer with a protease inhibitor cocktail. Cell lysates were centrifuged, then the supernatant fraction incubated with the anti-BCR-ABL antibody overnight at 4°C and subsequently with protein A magnetic beads (73778, Cell Signaling Technology) for another 4 h at 4°C. The bead complexes were washed three times with washing buffer (Tris 25 mM, NaCl 0.15 M, Tween-20 0.005%, pH 7.5), eluted with elution buffer (glycine 0.1 M, pH 2.0), and mixed with neutralization buffer (Tris 1 M, pH 9.0) for neutralization.

**Protein stability assay**

RAPSYN$^{WT}$, RAPSYN$^{Y336F}$, or BCR-ABL-transfected Ph$^{+}$ leukemia cells were incubated with 100 mg/mL cycloheximide (CHX, A8244; Cell Signaling Technology) for the indicated time points. Cells were harvested and lysed on ice using NP-40 lysis buffer supplemented with a protease inhibitor cocktail. The supernatant was collected and subjected to immunoblotting using anti-RAPSYN or SRC antibodies.

**Quantitative reverse transcription-PCR (RT-PCR)**

High-quality RNA was isolated from cells or tissues using Trizol reagent (AJF1807A, Takara) according to the manufacturer's instructions. cDNA was synthesized from 1 μg of total RNA using the HiScriptIIRT SuperMix for qPCR (R233-01, Vazyme). The ChamQ SYBR qPCR Master Mix (Q331-02, Vazyme) was used for two-step RT-PCR analysis on an Applied Biosystems StepOnePlus Real-Time PCR instrument. The samples were analyzed in triplicate. The expression value of the target gene in a given sample was normalized to the corresponding expression of ACTB or GAPDH. The 2-ΔΔCt method was used to calculate the relative expression of target genes. The primers used are listed in Supplemental Table S1.

**Cytotoxicity assay**

Lentiviruses co-expressing GFP were used to assess the toxicity of shRNAs. Flow cytometry was performed two days after shRNA transduction to determine the initial GFP-positive proportion of live cells for each shRNA. Subsequently, the cells were sampled every two days over time. The GFP-positive proportion at each time point was normalized to that of the day two. Each shRNA experiment was performed at least three times for each cell line.

**Statistical analysis**

All in vitro experiments were repeated at least three times. Animals were randomly assigned to different groups for each in vivo study. Kaplan-Meier survival analysis was used for all survival studies, and the log-rank test was used to determine significant differences between groups. Differences with * $p < 0.05$, ** $p < 0.01$, *** $p < 0.001$, and **** $p < 0.0001$ were considered significant. Prism 8 (GraphPad Software, CA, USA) was used for statistical analysis. Representative results from at least three independent replicates are shown. Data are

presented as the means ± SD, and significant differences were determined using the Student's t test, unpaired Student's t test, or one-way analysis of variance test.

**Acknowledgement**

This work was supported by grants from the National Key R&D Program of China (2018YFA0902000), the National Science Foundation of China (No. 81872924, 81973386 and 82002971), the "Double First-Class" University Project (CPU2022QZ014), the Project Program of the State Key Laboratory of Natural Medicines, China Pharmaceutical University (SKLNMZZ202201) and PAPD of Jiangsu Province.

**Additional information**

**Funding**

| Funder | Grant reference number | Author |
|---|---|---|
| National Natural Science Foundation of China | 81973386 | Yijun Chen |
| National Natural Science Foundation of China | 81872924 | Shuzhen Wang |
| National Natural Science Foundation of China | 82002971 | Beiying Dai |
| National Key R&D Program of China | 2018YFA0902000 | Yijun Chen |
| "Double First-Class" University Project | CPU2022QZ014 | Yijun Chen |
| Project Program of the State Key Laboratory of Natural Medicines | SKLNMZZ202201 | Yijun Chen |
| Key Research and Development Project of Guangdong Province | 2022B1111070004 | Yijun Chen |
| The funders had no role in the study design, data collection and interpretation, or the decision to submit the work for publication. | | |

## Author contributions

Mengya Zhao, Formal analysis, Investigation, Data curation, Methodology, Writing - original draft; Beiying Dai, Formal analysis, Investigation, Data curation, Methodology, Writing - original draft, Project administration, Funding acquisition; Xiaodong Li, Formal analysis, Investigation, Data curation, Methodology; Yixin Zhang, Formal analysis, Investigation, Data curation, Methodology; Chun Qiao, Data curation; Yaru Qin, Data curation; Qingmei Li, Data curation; Zhao Li, Data curation; Shuzhen Wang, Supervision, Project administration, Funding acquisition, Writing - review & editing; Yong Yang, Supervision, Resources; Yijun Chen, Conceptualization, Supervision, Resources, Writing - review & editing, Funding acquisition.

## Competing interests

A Chinese patent application was filed with the number of 202210107464.7. China Pharmaceutical University owns the patent rights, and Y. C., Y. Y., M. Z., B. D., X. L., S. W. and X. Z. are the inventors of the patent.

## Data availability

The data generated in this study are available upon request from the corresponding author.

## Ethics

This study was approved by the ethics committee of the First Affiliated Hospital of Nanjing Medical University (2019-SR-485.A1). All animal experiments were performed in accordance with the National Institutes of Health Guide for the Care and Use of Laboratory Animals with the approval of the Center for New Drug Evaluation and Research, China Pharmaceutical University (approval number: B20190925-1; Nanjing, China).

## Figures and figures legends

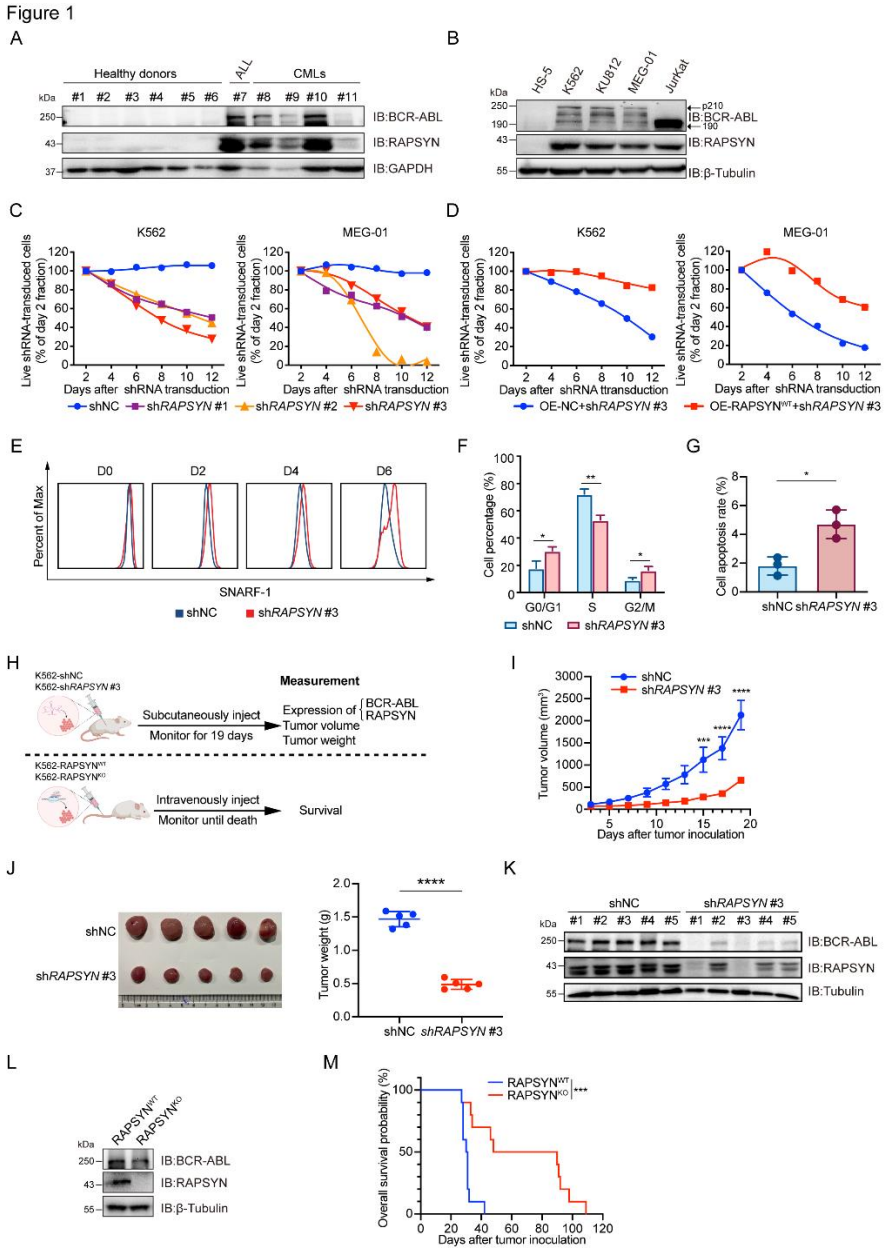


**Figure 1. High protein levels of RAPSYN promotes Ph⁺ leukemia progression.**

(A) Immunoblot of RAPSYN and BCR-ABL in the PBMCs of clinical samples.

(B) Immunoblots of RAPSYN and BCR-ABL in Ph⁺ leukemic cells and normal bone marrow stromal cells (HS-5).

(C) Cytotoxicity induced by shRNA-mediated RAPSYN knockdown in leukemic cells.

(D) Rescue of leukemic cells from sh*RAPSN* #3-induced toxicity by exogenous expression of RAPSN cDNA.

(E) Analysis of SNARF-1 labeling intensity in K562 cells transduced with shNC or

676 sh*RAPSN* #3.

677 (F) Quantification of cell cycle analyses in K562 cells transduced with shNC or

678 sh*RAPSN* #3.

679 (G) Quantification of cell apoptosis analyses in K562 cells transduced with shNC or

680 sh*RAPSN* #3.

681 (H) An in vivo experimental design for testing the effects of RAPSYN on tumor growth

682 and survival.

683 (I) The growth curve of subcutaneous xenograft tumors was measured every two days

684 from the third day after tumor inoculation for 19 days (five mice in each group).

685 (J) Photograph and weight quantification of excised tumor xenografts from (I).

686 (K) Immunoblot of RAPSYN and BCR-ABL in mouse xenograft tumor biopsies from

687 K562 cells transduced with sh*RAPSN* #3 or shNC.

688 (L) Immunoblot of RAPSYN and BCR-ABL in K562-RAPSYN$^{WT}$ and K562-RAPSYN$^{KO}$

689 cells.

690 (M) Kaplan-Meier survival curve of NCG mice following intravenous injection of K562-

691 RAPSYN$^{WT}$ or K562-RAPSYN$^{KO}$ cells, as shown in (H) (ten mice in each group).

692 All data represent the mean ± SD of at least three independent experiments. *P* values

693 were calculated using unpaired Student's t-test or log-rank test. * $p < 0.05$, ** $p <$

694 $0.01$, *** $p < 0.001$, **** $p < 0.0001$.

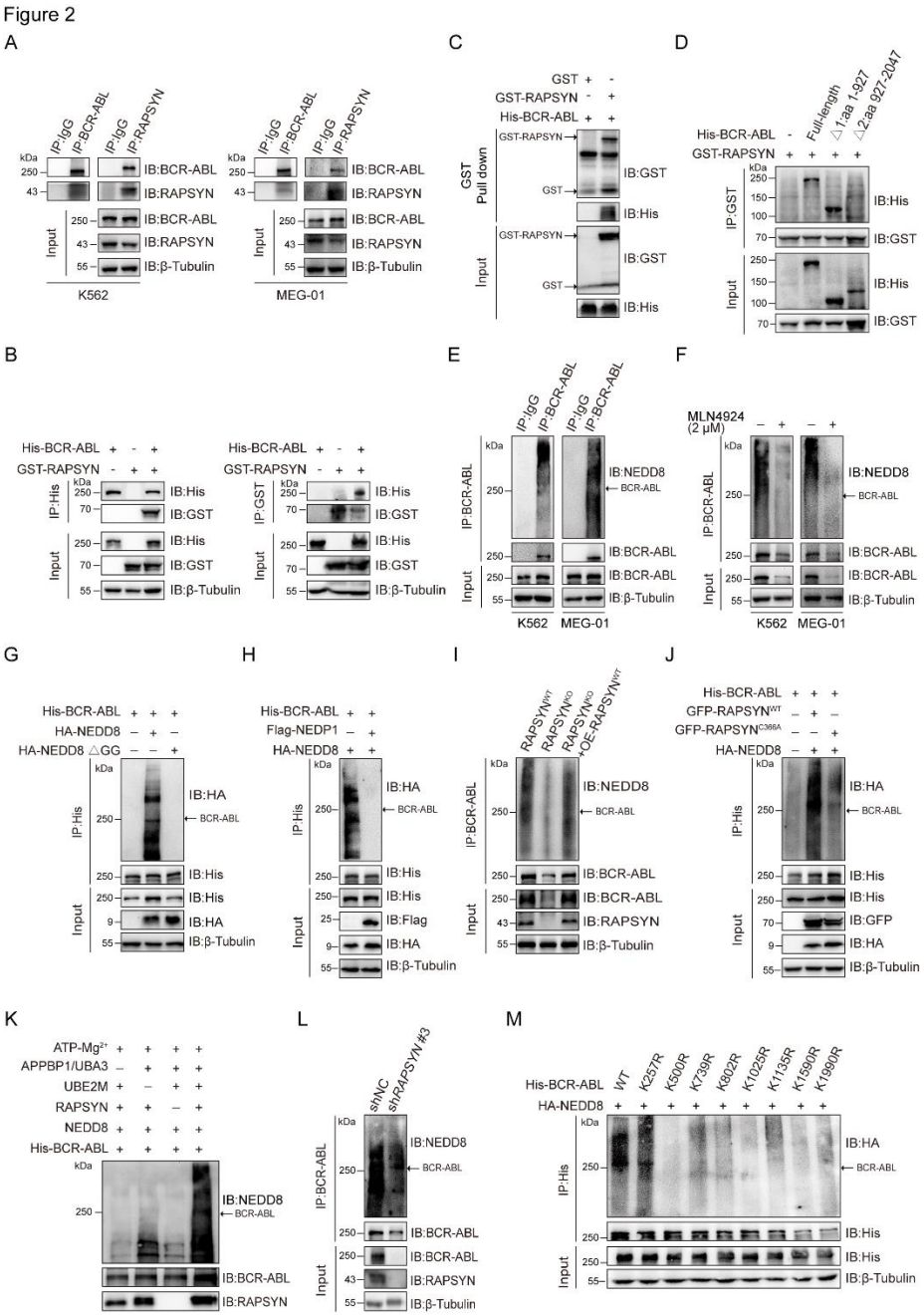


**Figure 2. RAPSYN neddylates BCR-ABL.**

(A) Co-immunoprecipitation of BCR-ABL and RAPSYN in leukemic cells.

(B) Immunoblot of GST and His after immunoprecipitation of His or GST in HEK293T cells transfected with His-tagged BCR-ABL and GST-tagged RAPSYN.

(C) Immunoblot of GST and His following GST pull-down after in vitro incubation of purified His-tagged BCR-ABL and GST or GST-tagged RAPSYN.

(D) His-immunoblot of GST immunoprecipitates from HEK293T cells transfected with GST-tagged RAPSYN alone or in combination with His-tagged full-length or truncated

704 BCR-ABL (Δ1: aa 1-927, Δ2: aa 928-2047).

705 (E) Analysis of BCR-ABL neddylation levels in leukemic cells.

706 (F) Analysis of BCR-ABL neddylation levels in leukemic cells treated with MLN4924 or
707 DMSO for 24 h.

708 (G) HA-immunoblot of His-immunoprecipitate from HEK293T cells transfected with
709 His-tagged BCR-ABL and HA-tagged NEDD8 or NEDD8 ΔGG.

710 (H) HA-immunoblot of the His-immunoprecipitate from HEK293T cells transfected with
711 the indicated constructs.

712 (I) Analysis of BCR-ABL neddylation levels in K562 WT, RAPSYN KO and RAPSYN
713 KO with exogenous expression of a RAPSN cDNA cells.

714 (J) HA-immunoblot after immunoprecipitation of His in HEK293T cells transfected with
715 His-tagged BCR-ABL, HA-tagged NEDD8, GFP-tagged WT RAPSYN or C366A
716 RAPSYN.

717 (K) Assessment of BCR-ABL neddylation by RAPSYN in vitro. Purified RAPSYN and
718 BCR-ABL were incubated with APPBP1/UBA3, UBE2M or NEDD8 in in vitro
719 neddylation assay.

720 (L) Analysis of BCR-ABL neddylation levels in excised tumor xenografts from Fig. 1J.

721 (M) Verification of BCR-ABL neddylation sites in HEK293T cells transfected with
722 indicated constructs.

723

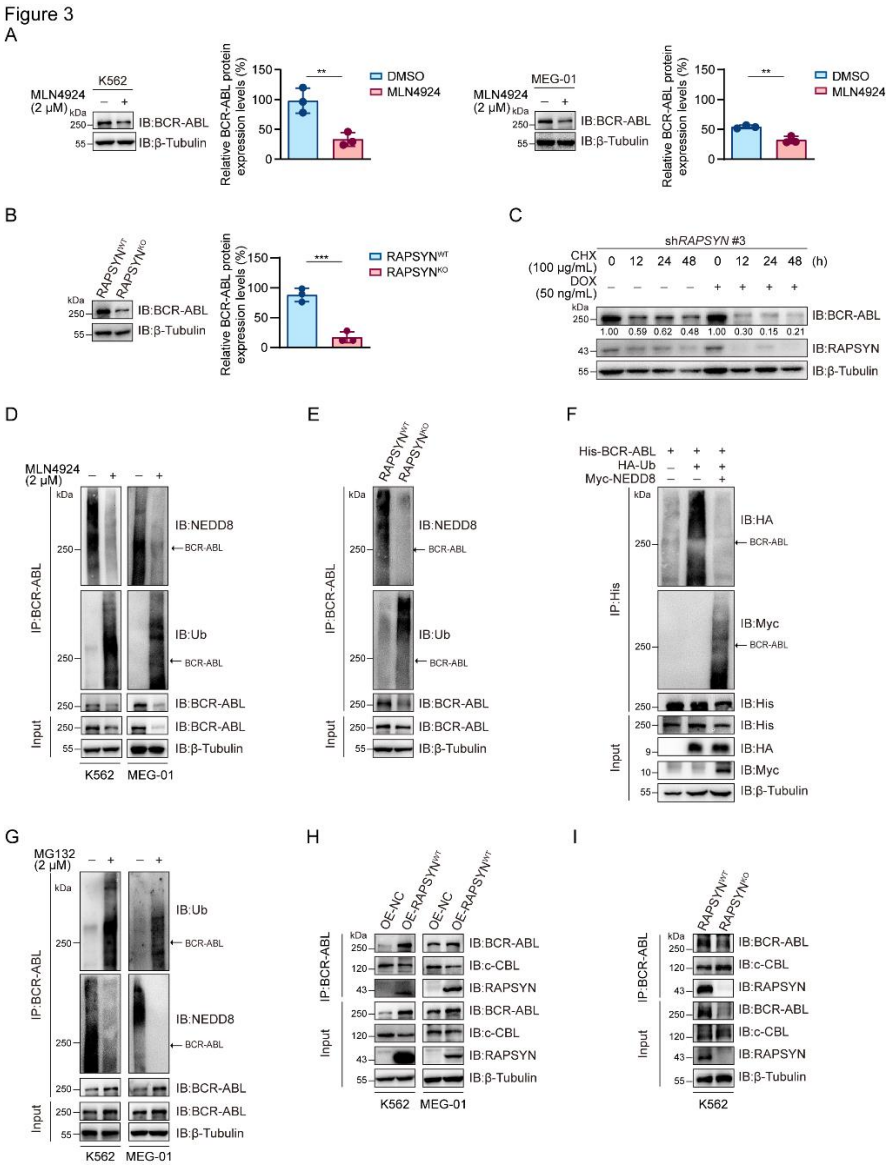


**Figure 3. RAPSYN attenuates BCR-ABL ubiquitination and degradation.**

(A) Immunoblot of BCR-ABL in leukemic cells treated with MLN4924 or DMSO for 24 h and corresponding quantification of three independent replicates.

(B) Immunoblot of BCR-ABL in K562 WT and RAPSYN KO cells and corresponding quantification of three independent replicates.

(C) Assessment of BCR-ABL protein stability in K562 cells expressing DOX-inducible sh*RAPSN* #3 treated with CHX alone or in combination with DOX at indicated time points by immunoblotting.

(D) Analysis of BCR-ABL neddylation and ubiquitination levels in leukemic cells treated with MLN4924 or DMSO for 24 h.

735 (E) Analysis of BCR-ABL neddylation and ubiquitination levels in K562 WT and
736 RAPSYN KO cells.
737 (F) Immunoblot of HA and Myc after His-immunoprecipitation in HEK293T cells
738 transfected with His-tagged BCR-ABL, HA-tagged Ub or without Myc-tagged NEDD8.
739 (G) Analysis of BCR-ABL ubiquitination and neddylation in leukemic cells treated with
740 MG132 or DMSO for 12 h.
741 (H) Co-immunoprecipitation of BCR-ABL, c-CBL and RAPSYN in leukemic cells
742 expressing exogenous RAPSN cDNA or empty vector.
743 (I) Co-immunoprecipitation of BCR-ABL, c-CBL and RAPSYN in K562 WT and
744 RAPSYN KO cells.
745 All data represent the mean ± SD of at least three independent experiments. P values
746 were calculated using unpaired Student's t-test. ** $p < 0.01$, *** $p < 0.001$.

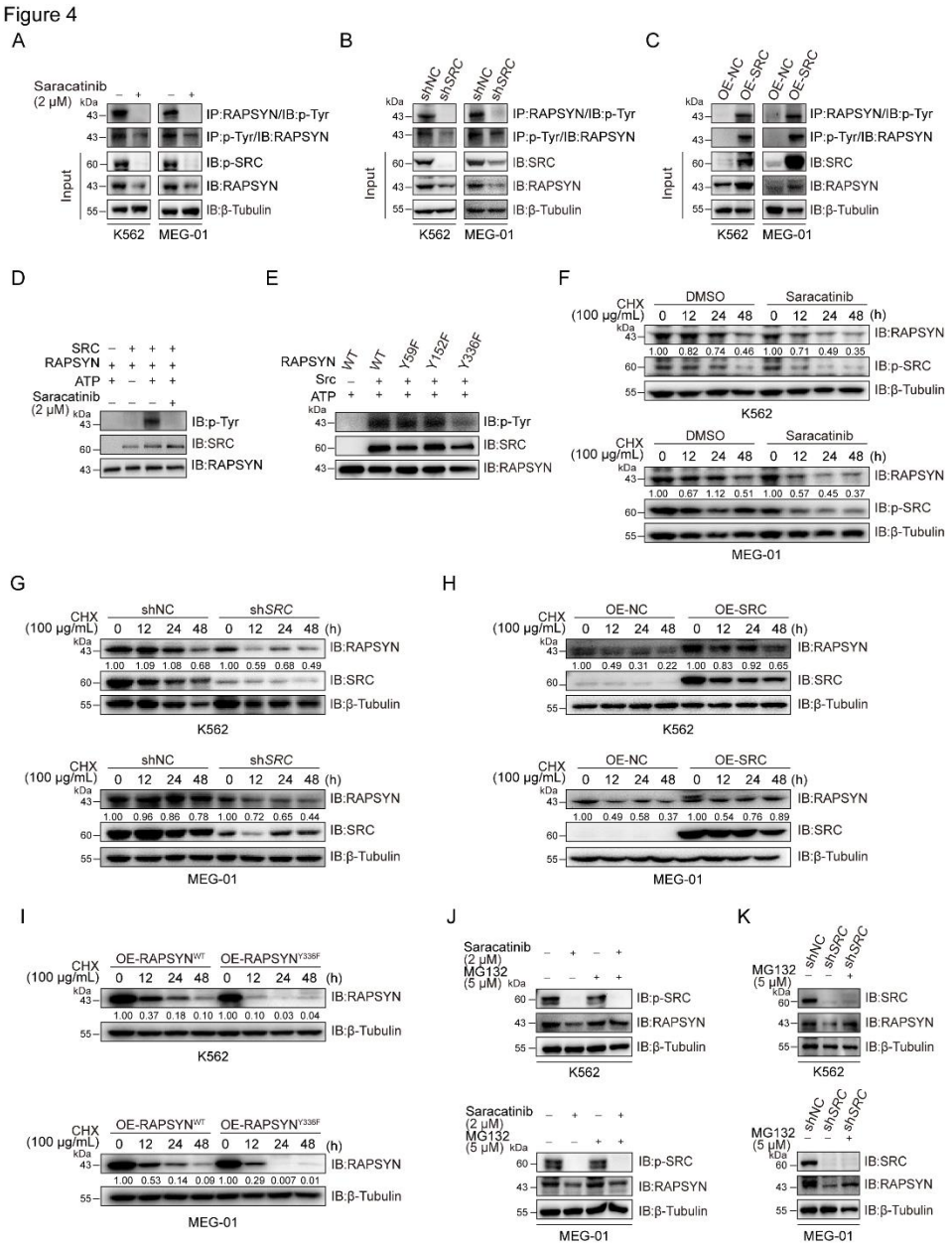


**Figure 4. SRC-mediated phosphorylation at Y336 promotes RAPSYN stability by repressing its proteasomal degradation.**

(A) Assessment of RAPSYN phosphorylation levels in leukemic cells treated with saracatinib or DMSO for 24 h.

(B) Assessment of RAPSYN phosphorylation levels in leukemic cells transduced with shSRC or shNC.

(C) Assessment of RAPSYN phosphorylation levels in leukemic cells expressing exogenous SRC cDNA or empty vector.

756 (D) Assessment of RAPSYN phosphorylation by SRC in vitro. Purified RAPSYN and
757 SRC were incubated with ATP in the presence or absence of saracatinib for
758 phosphorylation assay.
759 (E) Verification of RAPSYN phosphorylation sites. Purified SRC and RAPSYN WT or
760 indicated mutants were incubated with ATP for phosphorylation assay.
761 (F) Assessment of RAPSYN protein stability in leukemic cells treated with CHX in
762 combination with saracatinib or DMSO at indicated time points by immunoblotting.
763 (G) Assessment of RAPSYN protein stability in leukemic cells transduced with shSRC
764 or shNC by immunoblotting.
765 (H) Assessment of RAPSYN protein stability in leukemic cells transduced with
766 exogenous SRC cDNA or empty vector by immunoblotting.
767 (I) Assessment of RAPSYN protein stability in leukemic cells transduced with
768 exogenous RAPSYN WT or Y336F cDNA by immunoblotting.
769 (J) Immunoblot of RAPSYN in leukemic cells treated with saracatinib or DMSO for 12
770 h, and subsequently with MG132 or DMSO for another 12 h.
771 (K) Immunoblot of RAPSYN in leukemic cells transduced with shNC or shSRC and
772 treated with MG132 or DMSO for 12 h.

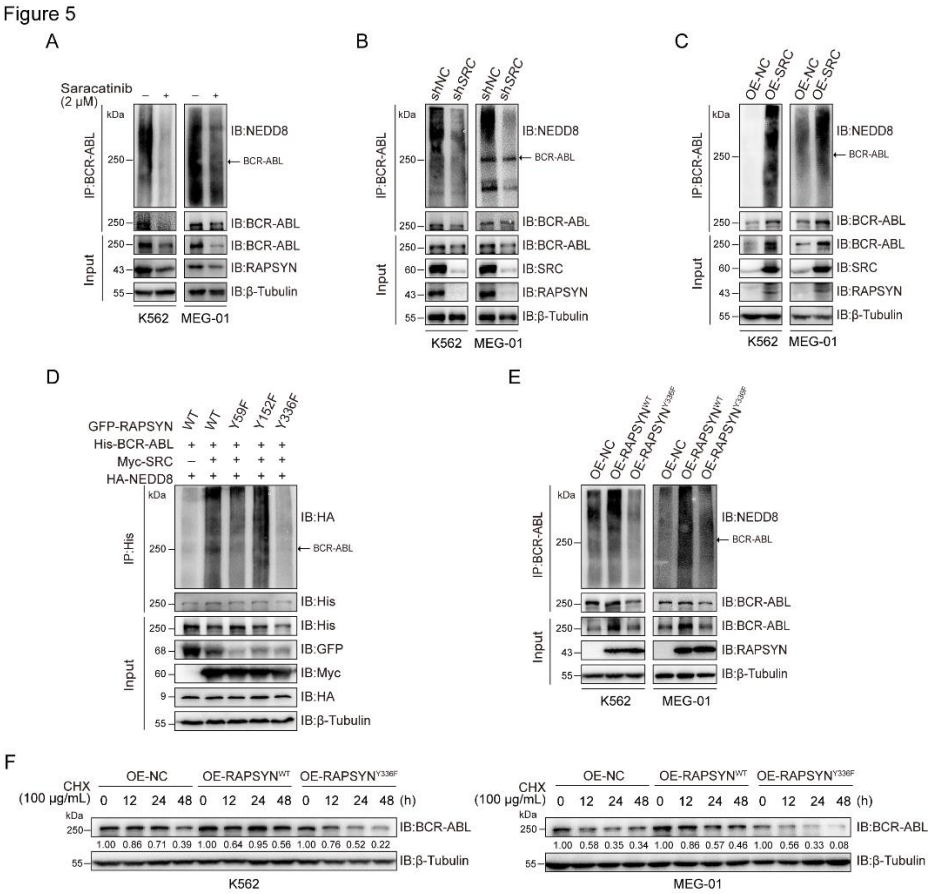


**Figure 5. RAPSYN phosphorylation at Y336 potentiates its E3 ligase activity and promotes BCR-ABL stabilization.**

(A) Immunoblot of BCR-ABL neddylation levels in leukemic cells treated with saracatinib or DMSO for 24 h.

(B) Immunoblot of BCR-ABL neddylation levels in leukemic cells transduced with sh*SRC* or shNC.

(C) Immunoblot of BCR-ABL neddylation levels in leukemic cells expressing exogenous SRC cDNA or empty vector.

(D) Effects of RAPSYN phosphorylation on BCR-ABL neddylation levels in HEK293T cells transfected with indicated constructs.

(E) Effects of RAPSYN phosphorylation at Y336 on BCR-ABL neddylation levels in leukemic cells expressing exogenous RAPSYN WT, Y336F cDNA, or empty vector.

(F) Assessment of BCR-ABL protein stability in leukemic cells transduced with exogenous RAPSYN WT, Y336F cDNA, or empty vector by immunoblotting.

Figure 6

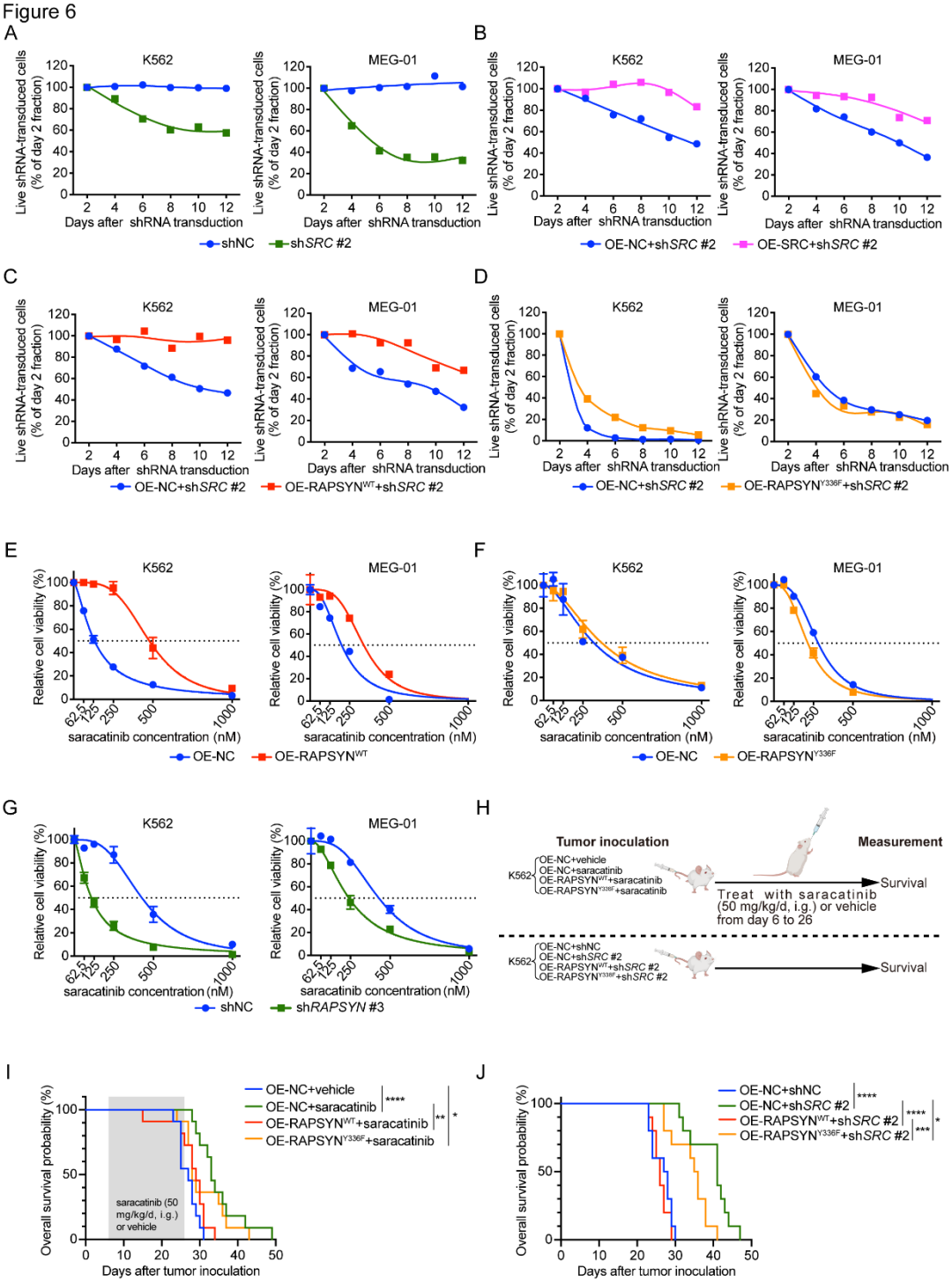


**Figure 6. SRC-mediated phosphorylation of RAPSYN at Y336 promotes Ph⁺ leukemia progression.**

(A) Cytotoxicity induced by sh*SRC* #2-mediated SRC knockdown in leukemic cells.

(B) Rescue of leukemic cells from sh*SRC* #2-induced toxicity by exogenous expression of SRC cDNA.

794 (C) Rescue of leukemic cells from sh*SRC* #2-induced toxicity by exogenous
795 expression of RAPSN$^{WT}$ cDNA.
796 (D) Failed rescue of leukemic cells from sh*SRC* #2-induced toxicity by exogenous
797 expression of RAPSN$^{Y336F}$ cDNA.
798 (E) Viability of leukemic cells transduced with either RAPSN$^{WT}$ cDNA or corresponding
799 empty vector after 72 h of incubation with indicated concentrations of saracatinib.
800 (F) Viability of leukemic cells transduced with either RAPSN$^{Y336F}$ cDNA or
801 corresponding empty vector after 72 h of incubation with indicated concentrations of
802 saracatinib.
803 (G) Viability of leukemic cells transduced with either shNC or sh*RAPSN* #3 after 72 h
804 of incubation with indicated concentrations of saracatinib.
805 (H) Experimental design used to test in vivo effects of RAPSYN phosphorylation at
806 Y336 on Ph$^{+}$ leukemia progression and survival time.
807 (I) Kaplan-Meier survival curve of NCG mice following intravenous injection of K562-
808 RAPSYN$^{WT}$ or K562-RAPSYN$^{Y336F}$ cells and intragastric administration of saracatinib
809 or corresponding vehicle from days 6 to 26 as indicated (ten mice in each group).
810 (J) Kaplan-Meier survival curve of NCG mice following intravenous injection of double-
811 transfected K562 cells (ten mice in each group). Representative results from at least
812 three independent experiments are shown (A-G); error bars, mean ± SD; * $p < 0.05$, **
813 $p < 0.01$, *** $p < 0.001$, **** $p < 0.0001$; log-rank test (I-L).
814
815
816
817
818
819
820

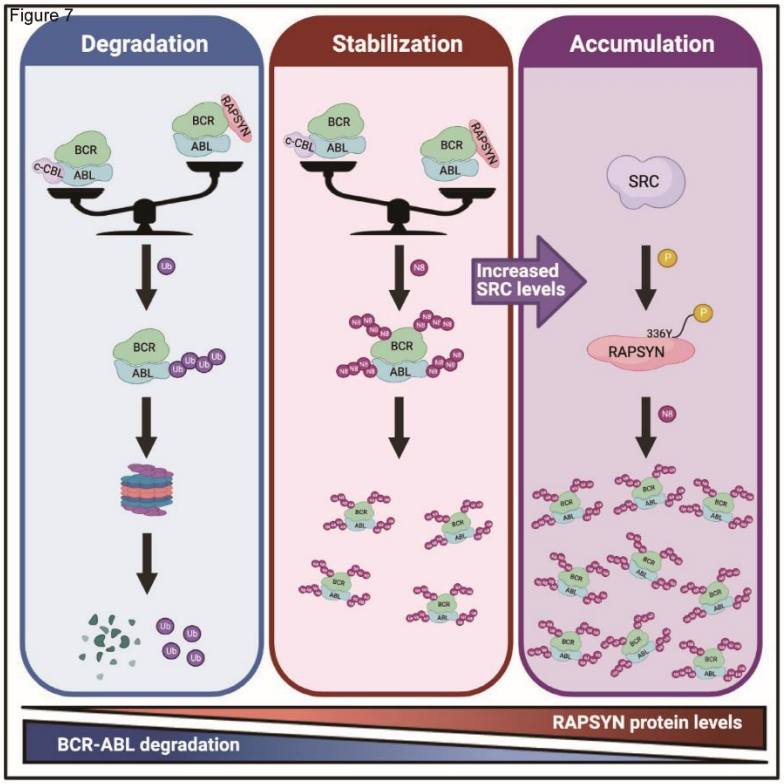


**Figure.7. Schematic representation of the competition between neddylation and ubiquitination on BCR-ABL in Ph⁺ leukemia.**

## Reference


Aydin, B., Kan, B., and Cabadak, H. 2013. The role of intracellular pathways in the proliferation of human K562 cells mediated by muscarinic receptors. *Leuk Res* ***37***: 1144-1149. DOI: 10.1016/j.leukres.2013.05.018.

Bahjat, M., de Wilde, G., van Dam, T., Maas, C., Bloedjes, T., Bende, R.J., van Noesel, C.J.M., Luijks, D.M., Eldering, E., Kersten, M.J., and Guikema, J.E.J. 2019. The NEDD8-activating enzyme inhibitor MLN4924 induces DNA damage in Ph+ leukemia and sensitizes for ABL kinase inhibitors. *Cell Cycle* ***18***: 2307-2322. DOI:10.1080/15384101.2019.1646068.

Barnes, D.J., Palaiologou, D., Panousopoulou, E., Schultheis, B., Yong, A.S., Wong, A., Pattacini, L., Goldman, J.M., and Melo, J.V. 2005. Bcr-Abl expression levels determine the rate of development of resistance to imatinib mesylate in chronic myeloid leukemia. *Cancer Res* ***65***: 8912-8919. DOI:10.1158/0008-5472.CAN-05-0076.

Bekes, M., Langley, D.R., and Crews, C.M. 2022. PROTAC targeted protein degraders: the past is prologue. *Nat Rev Drug Discov* ***21***: 181-200. DOI:10.1038/s41573-021-00371-6.

Braun, T.P., Eide, C.A., and Druker, B.J. 2020. Response and Resistance to BCR-ABL1-Targeted Therapies. *Cancer Cell* ***37***: 530-542. DOI:10.1016/j.ccell.2020.03.006.

Burslem, G.M., Schultz, A.R., Bondeson, D.P., Eide, C.A., Savage Stevens, S.L., Druker, B.J., and Crews, C.M. 2019. Targeting BCR-ABL1 in chronic myeloid leukemia by PROTAC-mmediated targeted protein degradation. *Cancer Res* ***79***: 4744-4753. DOI:10.1158/0008-5472.CAN-19-1236.

Cabadak, H., Aydin, B., and Kan, B. 2011. Regulation of M2, M3, and M4 muscarinic receptor expression in K562 chronic myelogenous leukemic cells by carbachol. *J Recept Signal Transduct Res* ***31***: 26-32. DOI:10.3109/10799893.2010.506484.

Cortes, J., Pavlovsky, C., and Saußele, S. 2021. Chronic myeloid leukaemia. *The Lancet* ***398***: 1914-1926. DOI:10.1016/s0140-6736(21)01204-6.

Deininger, M.W., Goldman, J.M., and Melo, J.V. 2000. The molecular biology of chronic myeloid leukemia. *Blood* ***96***: 3343-3356.

Demizu, Y., Shibata, N., Hattori, T., Ohoka, N., Motoi, H., Misawa, T., Shoda, T., Naito, M., and Kurihara, M. 2016. Development of BCR-ABL degradation inducers via the conjugation of an imatinib derivative and a cIAP1 ligand. *Bioorg Med Chem Lett* ***26***: 4865-4869. DOI:10.1016/j.bmcl.2016.09.041.

Durieux, M.E., and Nietgen, G.W. 1997. Synergistic inhibition of muscarinic signaling by ketamine stereoisomers and the preservative benzethonium chloride. *Anesthesiology* ***86***: 1326-1333. DOI:10.1097/00000542-199706000-00014.

Embade, N., Fernandez-Ramos, D., Varela-Rey, M., Beraza, N., Sini, M., Gutierrez de Juan, V., Woodhoo, A., Martinez-Lopez, N., Rodriguez-Iruretagoyena, B., Bustamante, F.J., de la Hoz, A.B., Carracedo, A., Xirodimas, D.P., Rodriguez, M.S., Lu, S.C., Mato, J.M., and Martinez-Chantar, M.L. 2012. Murine double minute 2 regulates Hu antigen R stability in human liver and colon cancer through NEDDylation. *Hepatology* ***55***: 1237-1248. DOI:10.1002/hep.24795.

Enchev, R.I., Schulman, B.A., and Peter, M. 2015. Protein neddylation: beyond cullin-RING ligases. *Nat Rev Mol Cell Biol* ***16***: 30-44. DOI:10.1038/nrm3919.

Guo, N., Azadniv, M., Coppage, M., Nemer, M., Mendler, J., Becker, M., and Liesveld, J. 2019. Effects of neddylation and mTOR Inhibition in acute myelogenous leukemia. *Transl Oncol* ***12***:

602-613. DOI:10.1016/j.tranon.2019.01.001.
Hochhaus, A., Baccarani, M., Silver, R.T., Schiffer, C., Apperley, J.F., Cervantes, F., Clark, R.E., Cortes, J.E., Deininger, M.W., Guilhot, F., Hjorth-Hansen, H., Hughes, T.P., Janssen, J., Kantarjian, H.M., Kim, D.W., Larson, R.A., Lipton, J.H., Mahon, F.X., Mayer, J., Nicolini, F., Niederwieser, D., Pane, F., Radich, J.P., Rea, D., Richter, J., Rosti, G., Rousselot, P., Saglio, G., Saussele, S., Soverini, S., Steegmann, J.L., Turkina, A., Zaritskey, A., and Hehlmann, R. 2020. European LeukemiaNet 2020 recommendations for treating chronic myeloid leukemia. *Leukemia* ***34***: 966-984. DOI:10.1038/s41375-020-0776-2.
Huh, K.H., and Fuhrer, C. 2002. Clustering of nicotinic acetylcholine receptors: from the neuromuscular junction to interneuronal synapses. *Mol Neurobiol* ***25***: 79-112. DOI:10.1385/MN:25:1:079.
Issaad, C., Ahmed, M., Novault, S., Bonnet, M.L., Bennardo, T., Varet, B., Vainchenker, W., and Turhan, A.G. 2000. Biological effects induced by variable levels of BCR-ABL protein in the pluripotent hematopoietic cell line UT-7. *Leukemia* ***14***: 662-670. DOI:10.1038/sj.leu.2401730.
Jabbour, E., Cortes, J., O'Brien, S., Giles, F., and Kantarjian, H. 2007. New targeted therapies for chronic myelogenous leukemia: opportunities to overcome imatinib resistance. *Semin Hematol* ***44***: S25-31. DOI:10.1053/j.seminhematol.2006.12.003.
Jabbour, E., and Kantarjian, H. 2020. Chronic myeloid leukemia: 2020 update on diagnosis, therapy and monitoring. *Am J Hematol* ***95***: 691-709. DOI:10.1002/ajh.25792.
Jakubik, J., Michal, P., Machova, E., and Dolezal, V. 2008. Importance and prospects for design of selective muscarinic agonists. *Physiol Res* ***57 Suppl 3***: S39-S47. DOI:10.33549/physiolres.931449.
Jiang, L., Wang, Y., Li, Q., Tu, Z., Zhu, S., Tu, S., Zhang, Z., Ding, K., and Lu, X. 2021a. Design, synthesis, and biological evaluation of Bcr-Abl PROTACs to overcome T315I mutation. *Acta Pharm Sin B* ***11***: 1315-1328. DOI:10.1016/j.apsb.2020.11.009.
Jiang, S., Wang, X., He, Y., Huang, H., Cao, B., Zhang, Z., Liu, J., Wang, Q., Huang, Z., and Mao, X. 2021b. Suppression of USP7 induces BCR-ABL degradation and chronic myelogenous leukemia cell apoptosis. *Cell Death Dis* ***12***: 456. DOI:10.1038/s41419-021-03732-6.
Bhalla KN, Fiskus W. 2016. NEDD8 and HDACs: promising cotargets in AML. *Blood* ***127***: 2167-2170. DOI:10.1182/blood-2016-02-699058.
Kawamata, J., Suzuki, S., and Shimohama, S. 2011. Enhancement of nicotinic receptors alleviates cytotoxicity in neurological disease models. *Ther Adv Chronic Dis* ***2***: 197-208. DOI:10.1177/2040622310397691.
Klein, A.d., Kessel, A.G.v., Grosveld, G., Bartram, C.R., Hagemeijer, A., Bootsma, D., Spurr, N.K., Heisterkamp, N., and J Groffen, J.R.S. 1982. A cellular oncogene is translocated to the Philadelphia chromosome in chronic myelocytic leukaemia. *Nature* ***300***: 765-767. DOI:10.1038/300765a0.
Lai, A.C., Toure, M., Hellerschmied, D., Salami, J., Jaime-Figueroa, S., Ko, E., Hines, J., and Crews, C.M. 2016. Modular PROTAC design for the degradation of oncogenic BCR-ABL. *Angew Chem Int Ed Engl* ***55***: 807-810. DOI:10.1002/anie.201507634.
Lee, G.W., Park, J.B., Park, S.Y., Seo, J., Shin, S.H., Park, J.W., Kim, S.J., Watanabe, M., and Chun, Y.S. 2018. The E3 ligase C-CBL inhibits cancer cell migration by neddylating the proto-oncogene c-Src. *Oncogene* ***37***: 5552-5568. DOI:10.1038/s41388-018-0354-5.
Legay, C., and Mei, L. 2017. Moving forward with the neuromuscular junction. *J Neurochem*

927 ***142 Suppl 2***: 59-63. DOI:10.1111/jnc.14028.
928 Li, J., Zou, J., Littlejohn, R., Liu, J., and Su, H. 2020. Neddylation, an emerging mechanism
929 regulating cardiac development and function. *Front Physiol* ***11***: 612927.
930 DOI:10.3389/fphys.2020.612927.
931 Li, L., Cao, Y., Wu, H., Ye, X., Zhu, Z., Xing, G., Shen, C., Barik, A., Zhang, B., Xie, X., Zhi, W.,
932 Gan, L., Su, H., Xiong, W.C., and Mei, L. 2016. Enzymatic activity of the scaffold protein rapsyn
933 for synapse formation. *Neuron* ***92***: DOI:1007-1019. 10.1016/j.neuron.2016.10.023.
934 Li, L., Xiong, W.C., and Mei, L. 2018. Neuromuscular junction formation, aging, and disorders.
935 *Annu Rev Physiol* ***80***: 159-188. 10.1146/annurev-physiol-022516-034255.
936 Li, X., and Song, Y. 2020. Proteolysis-targeting chimera (PROTAC) for targeted protein
937 degradation and cancer therapy. *J Hematol Oncol* ***13***: 50. DOI:10.1186/s13045-020-00885-3.
938 Liu, C., Nie, D., Li, J., Du, X., Lu, Y., Li, Y., Zhou, J., Jin, Y., and Pan, J. 2018. Antitumor effects
939 of blocking protein neddylation in T315I-BCR-ABL leukemia cells and leukemia stem cells.
940 *Cancer Res* ***78***: 1522-1536. DOI:10.1158/0008-5472.CAN-17-1733.
941 Liu, H., Mi, Q., Ding, X., Lin, C., Liu, L., Ren, C., Shen, S., Shao, Y., Chen, J., Zhou, Y., Ji, L.,
942 Zhang, H., Bai, F., Yang, X., Yin, Q., and Jiang, B. 2022. Discovery and characterization of
943 novel potent BCR-ABL degraders by conjugating allosteric inhibitor. *Eur J Med Chem* ***244***:
944 DOI:114810. 10.1016/j.ejmech.2022.114810.
945 Lussana, F., Intermesoli, T., Stefanoni, P., and Rambaldi, A. 2018. Mechanisms of resistance
946 to targeted therapies in chronic myeloid leukemia. *Handb Exp Pharmacol* ***249***: 231-250.
947 DOI:10.1007/164_2017_81.
948 Mao, J.H., Sun, X.Y., Liu, J.X., Zhang, Q.Y., Liu, P., Huang, Q.H., Li, K.K., Chen, Q., Chen, Z.,
949 and Chen, S.J. 2010. As4S4 targets RING-type E3 ligase c-CBL to induce degradation of BCR-
950 ABL in chronic myelogenous leukemia. *Proc Natl Acad Sci U S A* ***107***: 21683-21688.
951 DOI:10.1073/pnas.1016311108.
952 McGrail, D.J., Garnett, J., Yin, J., Dai, H., Shih, D.J.H., Lam, T.N.A., Li, Y., Sun, C., Li, Y.,
953 Schmandt, R., Wu, J.Y., Hu, L., Liang, Y., Peng, G., Jonasch, E., Menter, D., Yates, M.S., Kopetz,
954 S., Lu, K.H., Broaddus, R., Mills, G.B., Sahni, N., and Lin, S.Y. 2020. Proteome instability is a
955 therapeutic vulnerability in Mismatch Repair-Deficient cancer. *Cancer Cell* ***37***: 371-386 e312.
956 DOI:10.1016/j.ccell.2020.01.011.
957 Mohamed, A.S., and Swope, S.L. 1999. Phosphorylation and cytoskeletal anchoring of the
958 acetylcholine receptor by Src class protein-tyrosine kinases. Activation by rapsyn. *J Biol Chem*
959 ***274***: 20529-20539. DOI:10.1074/jbc.274.29.20529.
960 Norton, J.P., Augert, A., Eastwood, E., Basom, R., Rudin, C.M., and MacPherson, D. 2021.
961 Protein neddylation as a therapeutic target in pulmonary and extrapulmonary small cell
962 carcinomas. *Genes Dev* ***35***: 870-887. DOI:10.1101/gad.348316.121.
963 Önder Narin G., Aydin, B., and Cabadak, H. 2021. Studies on the role of alpha 7 nicotinic
964 acetylcholine receptors in K562 cell proliferation and signaling. *Mol Biol Rep* ***48***: 5045-5055.
965 DOI:10.1007/s11033-021-06498-4.
966 Oved, S., Mosesson, Y., Zwang, Y., Santonico, E., Shtiegman, K., Marmor, M.D.,
967 Kochupurakkal, B.S., Katz, M., Lavi, S., Cesareni, G., and Yarden, Y. 2006. Conjugation to
968 Nedd8 instigates ubiquitylation and down-regulation of activated receptor tyrosine kinases. *J*
969 *Biol Chem* ***281***: 21640-21651. DOI:10.1074/jbc.M513034200.
970 Shibata, N., Ohoka, N., Tsuji, G., Demizu, Y., Miyawaza, K., Ui-Tei, K., Akiyama, T., and Naito,

M. 2020. Deubiquitylase USP25 prevents degradation of BCR-ABL protein and ensures proliferation of Ph-positive leukemia cells. *Oncogene* ***39***: 3867-3878. DOI:10.1038/s41388-020-1253-0.

Shimokawa, K., Shibata, N., Sameshima, T., Miyamoto, N., Ujikawa, O., Nara, H., Ohoka, N., Hattori, T., Cho, N., and Naito, M. 2017. Targeting the allosteric site of oncoprotein BCR-ABL as an alternative strategy for effective target protein degradation. *ACS Med Chem Lett* ***8***: 1042-1047. DOI:10.1021/acsmedchemlett.7b00247.

van der Veen, A.G., and Ploegh, H.L. 2012. Ubiquitin-like proteins. *Annu Rev Biochem* ***81***: 323-357. DOI:10.1146/annurev-biochem-093010-153308.

Wang, S., Xie, W., Wang, D., Peng, Z., Zheng, Y., Liu, N., Dai, W., Wang, Y., Wang, Z., Yang, Y., and Chen, Y. 2015. Discovery of a small molecule targeting SET-PP2A interaction to overcome BCR-ABL$^{T315I}$ mutation of chronic myeloid leukemia. *Oncotarget* ***6***: 12128-12140. DOI:10.18632/oncotarget.3665.

Witzemann, V., Chevessier, F., Pacifici, P.G., and Yampolsky, P. 2013. The neuromuscular junction: selective remodeling of synaptic regulators at the nerve/muscle interface. *Mech Dev* ***130***: 402-411. DOI:10.1016/j.mod.2012.09.004.

Xie, P., Peng, Z., Chen, Y., Li, H., Du, M., Tan, Y., Zhang, X., Lu, Z., Cui, C.P., Liu, C.H., He, F., and Zhang, L. 2021. Neddylation of PTEN regulates its nuclear import and promotes tumor development. *Cell Res* ***31***: 291-311. DOI:10.1038/s41422-020-00443-z.

Xing, G., Jing, H., Zhang, L., Cao, Y., Li, L., Zhao, K., Dong, Z., Chen, W., Wang, H., Cao, R., Xiong, W.C., and Mei, L. 2019. A mechanism in agrin signaling revealed by a prevalent Rapsyn mutation in congenital myasthenic syndrome. *eLlife* ***8***. DOI:10.7554/eLife.49180.

Xing, G., Xiong, W.C., and Mei, L. 2020. Rapsyn as a signaling and scaffolding molecule in neuromuscular junction formation and maintenance. *Neurosci Lett* ***731***: 135013. DOI:10.1016/j.neulet.2020.135013.

Yang, Y., Ding, L., Guo, Z.K., Zheng, X.L., Wang, L.S., Sun, H.Y., Jin, Z.G., and Wang, H.X. 2017. The epigenetically-regulated miR-34a targeting c-SRC suppresses RAF/MEK/ERK signaling pathway in K-562 cells. *Leuk Res* ***55***: 91-96. DOI:10.1016/j.leukres.2017.01.020.

Yao, J., Liang, X., Liu, Y., and Zheng, M. 2020. Neddylation: A Versatile Pathway Takes on Chronic Liver Diseases. *Front Med (Lausanne)* ***7***: 586881. DOI:10.3389/fmed.2020.586881.

Ying, J., Zhang, M., Qiu, X., and Lu, Y. 2018. Targeting the neddylation pathway in cells as a potential therapeutic approach for diseases. *Cancer Chemother Pharmacol* ***81***: 797-808. DOI:10.1007/s00280-018-3541-8.

Zhao, Q., Ren, C., Liu, L., Chen, J., Shao, Y., Sun, N., Sun, R., Kong, Y., Ding, X., Zhang, X., Xu, Y., Yang, B., Yin, Q., Yang, X., and Jiang, B. 2019. Discovery of SIAIS178 as an effective BCR-ABL degrader by recruiting Von Hippel-Lindau (VHL) E3 ubiquitin ligase. *J Med Chem* ***62***: 9281-9298. 10.1021/acs.jmedchem.9b01264.

Zhou, L., Chen, S., Zhang, Y., Kmieciak, M., Leng, Y., Li, L., Lin, H., Rizzo, K.A., Dumur, C.I., Ferreira-Gonzalez, A., Rahmani, M., Povirk, L., Chalasani, S., Berger, A.J., Dai, Y., and Grant, S. 2016. The NAE inhibitor pevonedistat interacts with the HDAC inhibitor belinostat to target AML cells by disrupting the DDR. *Blood* ***127***: 2219-2230. DOI:10.1182/blood-2015-06-653717.

Zhou, L., Jiang, Y., Luo, Q., Li, L., and Jia, L. 2019. Neddylation: a novel modulator of the tumor microenvironment. *Mol Cancer* ***18***: 77. DOI:10.1186/s12943-019-0979-1.

Zhou, Q., and Sun, Y. 2019. MLN4924: additional activities beyond neddylation inhibition. *Mol*

1015 *Cell Oncol* ***6***: e1618174. DOI:10.1080/23723556.2019.1618174.
1016 Zuo, W., Huang, F., Chiang, Y.J., Li, M., Du, J., Ding, Y., Zhang, T., Lee, H.W., Jeong, L.S.,
1017 Chen, Y., Deng, H., Feng, X.H., Luo, S., Gao, C., and Chen, Y.G. 2013. c-Cbl-mediated
1018 neddylation antagonizes ubiquitination and degradation of the TGF-beta type II receptor. *Mol*
1019 *Cell* ***49***: 499-510. DOI:10.1016/j.molcel.2012.12.002.
1020